Structure−Activity Profiles of Complex Biantennary Glycans with Core Fucosylation and with/without Additional α2,3/α2,6 Sialylation: Synthesis of Neoglycoproteins and Their Properties in Lectin Assays, Cell Binding, and Organ Uptake†

Carlo Unverzagt,*,‡ Sabine André,§ Joachim Seifert,‡ Shuji Kojima,|| Christian Fink,⊥ Geetha Srikrishna,# Hudson Freeze,# Klaus Kayser,⊥ and Hans-Joachim Gabius§

Institut für Organische Chemie und Biochemie, Technische Universität München, Lichtenbergstrasse 4, 85748 Garching, Germany, Institut für Physiologische Chemie, Tierärztliche Fakultät, Ludwig-Maximilians-Universität München, Veterinärstrasse 13, 80539 München, Germany, Research Institute for Biological Sciences, Science University of Tokyo, Yamazaki 2669, Noda-City, Chiba 278, Japan, Abteilung Pathologie, Thoraxklinik, Amalienstrasse 5, 69126 Heidelberg, Germany, and The Burnham Institute, 10901 North Torrey Pines Road, La Jolla, California 92037

Received August 17, 2001

The consideration of oligosaccharides and glycoconjugates as biopharmaceuticals is an emerging topic in drug design. Chemoenzymatic synthesis of *N*-glycans was performed to examine the influence of *N*-glycan core fucosylation on lectin-binding properties and biodistribution. As a first step in a systematic comparison of *N*-glycans, the core fucose moiety was chemically introduced into a complex-type biantennary heptasaccharide azide. After deprotection and attachment of a spacer, the terminal sections of the *N*-glycan were elongated enzymatically. Conversion of the amino group in the spacer to an isothiocyanate gave derivatives allowing convenient ligand attachment to bovine serum albumin (BSA). The resulting neoglycoproteins contained an average of 2.9−4.6 chains per carrier molecule. Relative to unsubstituted biantennary complex-type *N*-glycans, the core fucosylation appears to favor the extended orientation of the α1,6-arm. This was deduced from an up to 5-fold alteration of affinity for lectins in solid-phase assays. Marked differences were also found for cell surface binding of cultured tumor cells, for staining of tumor cells in lung sections, and in organ distribution. In vivo, the α2,6-sialylated neoglycoproteins showed a reduced serum half-life in mice relative to the α2,3-sialylated isomer and the non-fucosylated congeners. These results support the notion that changing the shape of a glycan provides a promising strategy to optimize the affinity of protein−carbohydrate interactions. Overall, our study underscores the importance of chemoenzymatic synthesis to define the effect of chain orientation on the ligand properties of *N*-glycans.

Introduction

Protein(lectin)−carbohydrate recognition owes its wide range of potential medical applications to several factors. They include the enormous information-storing capacity of the sugar code, the ubiquitous presence of cellular glycoconjugates with often distinctly tailored glycan parts, and the matching presence of complementary receptors homing in on selected carbohydrate epitopes.[1−5] For optimal results, drug design in this area will have to consider the entire spectrum of structural aspects of ligands. Suitably designed panels of oligosaccharides have considerably accelerated the delineation of sequence features crucial for enhancing affinity (e.g., linkage points and substitution patterns). However, the topological presentation of carbohydrate determinants also affects the affinity for binding sites. With single contacts often being rather weak, a dense arrangement of epitopes forming mini- or maxiclusters can lead to dissociation constants in the low nanomolar range and even beyond. In polyvalent interaction systems, high-affinity binding was observed with tissues, bacterial or viral lectins, the hepatic C-type asialoglycoprotein receptor serving as role model.[6−9]

Biological recognition can thus be modulated profoundly by the density and accessibility of carbohydrate ligands. This potential of adjustable binding affinity should be exploited in drug design. Therefore, we commenced a systematic study of the relationship between structure and molecular recognition involving *N*-glycans attached to an inert protein backbone (neoglycoprotein). Information obtained in these studies is expected to reveal functional implications of glycan microheterogeneity in natural glycoproteins. This line of investigation was started with neoglycoproteins carrying ovalbumin-derived high-mannose-type *N*-glycans.[10] After complex-type biantennary *N*-glycans became accessible by chemoenzymatic total synthesis, their ligand properties in neoglycoproteins were examined.[11,12] As a next step, it was desirable to assess the impact of typical

† Dedicated to Prof. Joachim Thiem on the occasion of his 60th birthday.

* To whom correspondence should be addressed. Current address: Bioorganische Chemie, Universität Bayreuth, Gebäude NW1, 95440 Bayreuth, Germany. Phone: +49-921-552670. Fax: +49-921-555365. E-mail: carlo.unverzagt@uni-bayreuth.de.
‡ Technische Universität München.
§ Ludwig-Maximilians-Universität München.
|| Science University of Tokyo.
⊥ Thoraxklinik.
The Burnham Institute.

10.1021/jm0110237 CCC: $22.00
Published on Web 12/20/2001

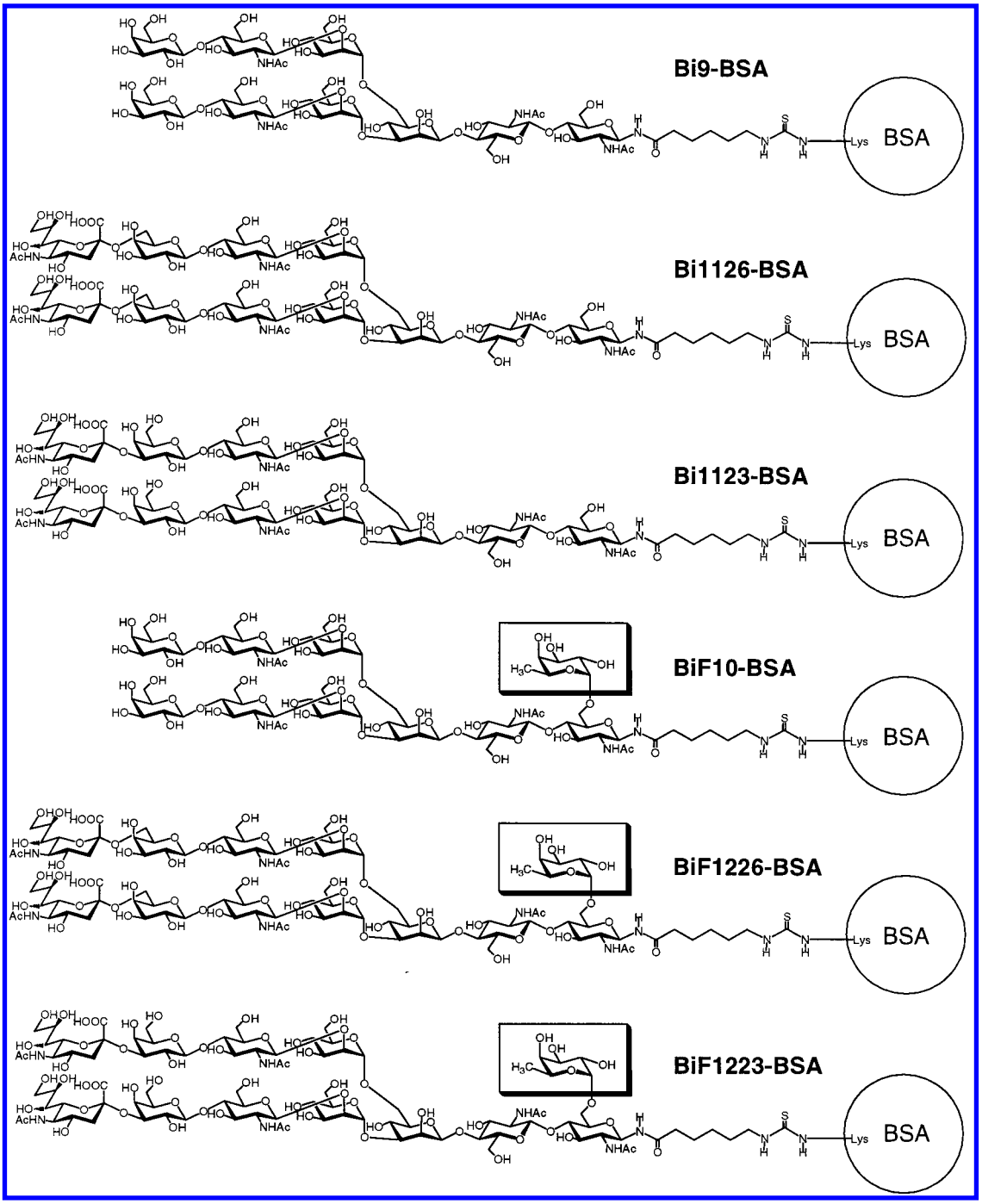

Figure 1. Neoglycoproteins with bovine serum albumin (BSA) as carrier for the test panel of six complex-type biantennary *N*-glycans. The abbreviation BiF1226-BSA stands for *bi*antennary core-*f*ucosylated *N*-glycan *12*-mer α*2,6*-sialylated *BSA* conjugate. The linker arm and the attachment point to an ϵ-amino group of lysine on the carrier protein are also shown.

modifications of the basic biantennary structure on the binding characteristics of sugar receptors (lectins and antibodies).

The common core structure of *N*-glycans encompasses two branches at the central mannose unit: the α1,3- and the α1,6-arm (Figure 1). It is important to consider the flexibility of each antenna, which correlates to the conformational entropy of the ligand and influences the free energy of binding to a receptor. Remarkably, computational and experimental studies have delineated a pronounced sensitivity of the populated conformational space of the α1,6-arm to the presence of substituents.[13−15] The addition of the α1,6-linked core fucose moiety will significantly shift the equilibrium between extended and folded orientations of the α1,6-arm to the extended form, presumably by a steric blocking effect.[16−19] Biologically, the presence of a core fucosyl moiety is a key recognition feature for polysialylation of mouse neural cell adhesion molecule and a regulatory attribute for de-N-glycosylation by mammalian, but not plant or bacterial, *N*-glycanases. Core fucosylation is also a decisive factor for the acquisition of low-malignant properties of human Hep3B hepatoma cells in culture and a regulator in chicken retina spheroid proliferation and organization.[20−23] Phenomenologically, increased α1,6-fucosyltransferase activity

has been reported in hepatoma and, to a lesser extent, in chronic hepatitis and liver cirrhosis.[24] Thus, the biological relevance of an α1,6-core fucosyl moiety in *N*-glycans warrants model studies to define its influence on carbohydrate recognition.

In this study, we describe the chemoenzymatic synthesis of activated derivatives of biantennary core-fucosylated *N*-glycans and their efficient conjugation to bovine serum albumin (BSA) to produce a panel of neoglycoproteins. The ligand properties of the glycans were determined and compared to a homologous set of neoglycoproteins differing only in the core fucosyl moiety. For this analysis the basic chemical properties of the two sets of neoglycoproteins with respect to glycan density or the type of spacer were deliberately kept constant. The ligand structures of the six tested neoglycoproteins together with the used nomenclature are shown in Figure 1. Besides localizing carbohydrate binding sites by glycohistochemistry, the histopathological work in lung cancer included monitoring of core-fucosylated *N*-glycans on the specimen using a monoclonal antibody against the core-fucosylated epitope.[25]

Chemistry

The total synthesis of complete *N*-glycans is an ongoing challenge[26] in order to generate sufficient quantities of these compounds for biological testing. The combined chemical and enzymatic approach developed for this purpose[11] affords several advantages over the traditional strategy that is relying solely on the isolation of *N*-glycans from natural sources.[27] In principle, the chemical synthesis can be scaled up to the quantity desired, leading to pure and homogeneous products. Additionally, the requirement for chemical attachment of linkers or other modes of conjugation can be readily accommodated during the course of the synthesis. We have prepared a set of modular building blocks[28] to assemble the most common *N*-glycan cores. To obtain related or novel structures not yet covered by the available *N*-glycan fragments, only single building blocks or segments of the synthesis need to be newly devised.[29] Final extension of the deprotected *N*-glycans can be accomplished by glycosyltransferases giving rapid access to typical and biologically relevant determinants.

The chemical synthesis of the core-fucosylated octasaccharide **1**, which is shown in Figure 2, was performed as outlined before.[30] Compound **1** was obtained after sequential deprotection of the corresponding core-fucosylated octasaccharide precursor. To facilitate subsequent conjugation of the *N*-glycan to proteins via a chemically stable spacer, the azido function at the anomeric center of compound **1** was reduced and coupled to *N*-benzyloxycarbonyl-6-aminohexanoic acid **2** (Z-AH-OH). Selective reduction of the azide was accomplished by reaction with propane-1,3-dithiol[31] in methanol. After removal of the volatiles, the remaining amine was acylated with the aminohexanoic acid derivative **2** preactivated with TBTU/HOBt. The resulting spacer-linked octasaccharide **3** was obtained in 52% yield after purification by reversed-phase HPLC. Catalytic hydrogenation cleaved the four benzylic protective groups, giving the free octasaccharide conjugate **4**. The water-soluble octasaccharide **4** contains two terminal GlcNAc residues at the nonreducing end that serve as acceptors for chain elongation by galactosyltransferase. The enzyme transfers a β1,4-linked galactose residue to each of the antennae, producing the galactosylated decasaccharide **5** in 75% yield after purification. Introduction of terminal sialic acid residues was accomplished by incubation of the crude reaction mixture (**5**) with CMP-sialic acid and either α2,6-sialyltransferase or α2,3-sialyltransferase furnishing the sialylated dodecasaccharides **6** and **7** (Figure 2). Enzymatic elongations were carried out in the presence of alkaline phosphatase to limit the inhibition of the transferases by nucleoside-phosphates.[32] All compounds were structurally characterized by electrospray mass spectrometry and state of the art 2D-NMR techniques comprising correlation spectroscopy (COSY), total correlation spectroscopy (TOCSY), nuclear Overhauser effect spectroscopy (NOESY), heteronuclear multiple-quantum coherence (HMQC), and HMQC−COSY experiments,[33] allowing the full assignment of the ring carbons and hydrogens at all steps of the reaction pathway.

Synthesis of the neoglycoproteins was performed via activation of the terminal amino function in the spacer of the three *N*-glycans **5**, **6**, and **7** (Figure 3). Conversion to the isothiocyanate proceeded smoothly by addition of thiophosgene in a biphasic reaction.[34] The freshly activated *N*-glycans (10 equiv) were coupled to carbohydrate-free bovine serum albumin at pH 9.0. Incorporation of the *N*-glycans was determined by a colorimetric assay[35] showing that the biantennary decasaccharide averaged 3.9 chains per BSA molecule, the α2,3-sialylated dodecasaccharide gave 4.6 chains, and the α2,6-sialylated compound yielded 2.9 chains. These results were in agreement with the electrophoretic mobilities of the three neoglycoproteins, i.e., BiF10-BSA, BiF1223-BSA, and BiF1226-BSA (*bi*antennary core-*f*ucosylated *N*-glycan *12*-mer α*2,6*-sialylated *BSA* conjugate) (see Figure 1), compared to underivatized BSA.

Biochemistry, Cell Biology, and Histopathology

Following the synthesis of the neoglycoproteins, their biological activity and application as diagnostic agents were tested with sugar receptors, cultured tumor cell lines, and tissue sections of cancer cases. The affinity of three structurally nonhomologous galactose-specific proteins to the core-fucosylated *N*-glycans of the three synthetic neoglycoproteins was analyzed in a solid-phase assay. Binding of the labeled sugar receptor to the surface-immobilized neoglycoprotein was determined at different marker concentrations up to saturation. From these binding data the dissociation constants in this system were determined. By use of a panel of 13 human tumor cell lines (leukemia/lymphoma, carcinoma and melanoma lines), the pharmacologically relevant binding to the neoglycoproteins was quantitated in vitro by flow cytofluorometry. The kinetics of organ distribution were monitored in vivo after iv injection of the iodinated neoglycoproteins into mice. Sections of various types of lung cancer were fixed and processed glycohistochemically to compare staining of the Bi and BiF-BSA conjugates (Figure 1) and to delineate differential binding properties useful for tumor diagnosis.

Results and Discussion

To carry out glycobiological studies with neoglycoproteins bearing chemically homogeneous oligosaccharides,

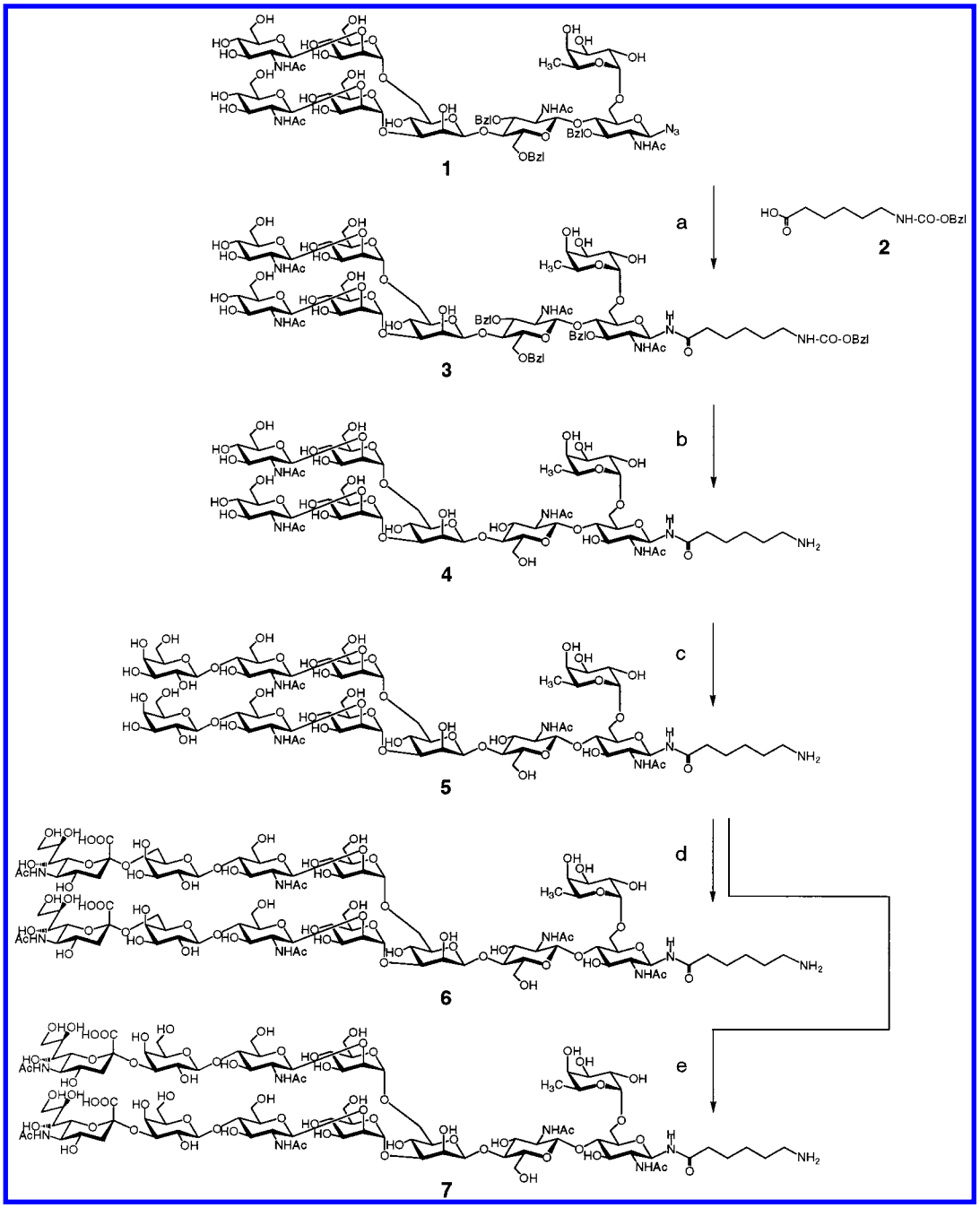

Figure 2. Chemical and enzymatic transformations to produce core-fucosylated galactosylated and sialylated *N*-glycans: (a) (1) propanedithiol, Et_3N, MeOH, (2) *N*-benzyloxycarbonyl-6-aminohexanoic acid **2**, TBTU, 1-hydroxybenzotriazole (HOBt) (1.0−2.0, 52%); (b) Pd/H_2, AcOH, MeOH (92%); (c) β1,4-galactosyltransferase, UDP-Gal, alkaline phosphatase (75%); (d) α2,6-sialyltransferase, CMP-NeuNAc, alkaline phosphatase (steps c + d, 62%); (e) α2,3-sialyltransferase, CMP-NeuNAc, alkaline phosphatase (steps c + e, 63%).

N-glycans were prepared by a combined chemical and enzymatic approach starting from the octasaccharide azide **1** (Figure 2). Selective reduction and introduction of the spacer *N*-benzyloxycarbonyl-6-aminohexanoic acid **2** set the stage for product purification by reversed-phase HPLC, taking advantage of the presence of four benzylic protective groups. Following deprotection, the outer carbohydrate chains were enzymatically elongated to the galactosylated or sialylated *N*-glycans **5**−**7** (Figure 2). To facilitate coupling to the protein, an isothiocyanate was generated at the spacer of the *N*-glycans, which subsequently reacted with free ϵ-NH_2 groups of the carrier (Figure 3). This convenient procedure, established to synthesize carbohydrate immunogens by conjugating *p*-aminophenyl glycosides to proteins,[34] can also be used for the conjugation of nonprotein carriers. The coupling density will depend not only on the accessibility of the acceptor groups but also on the steric bulk of the carbohydrate chains. In contrast to mono- and disaccharides large *N*-glycans cannot be conjugated to albumin with yields in the range of 20−30 substituents per molecule. In fact, the average molar ratio of glycan to carrier was 3.9 for the decasaccharide **5** and 2.9 (**6**) and 4.6 (**7**) for the two dodecasaccharides (Figure 1, lower part). Since the yields of incorporation were similar to those obtained with unsubstituted *N*-glycans,[12] the presence of a core fucosyl unit in the vicinity of the spacer did not impair glycan attachment to

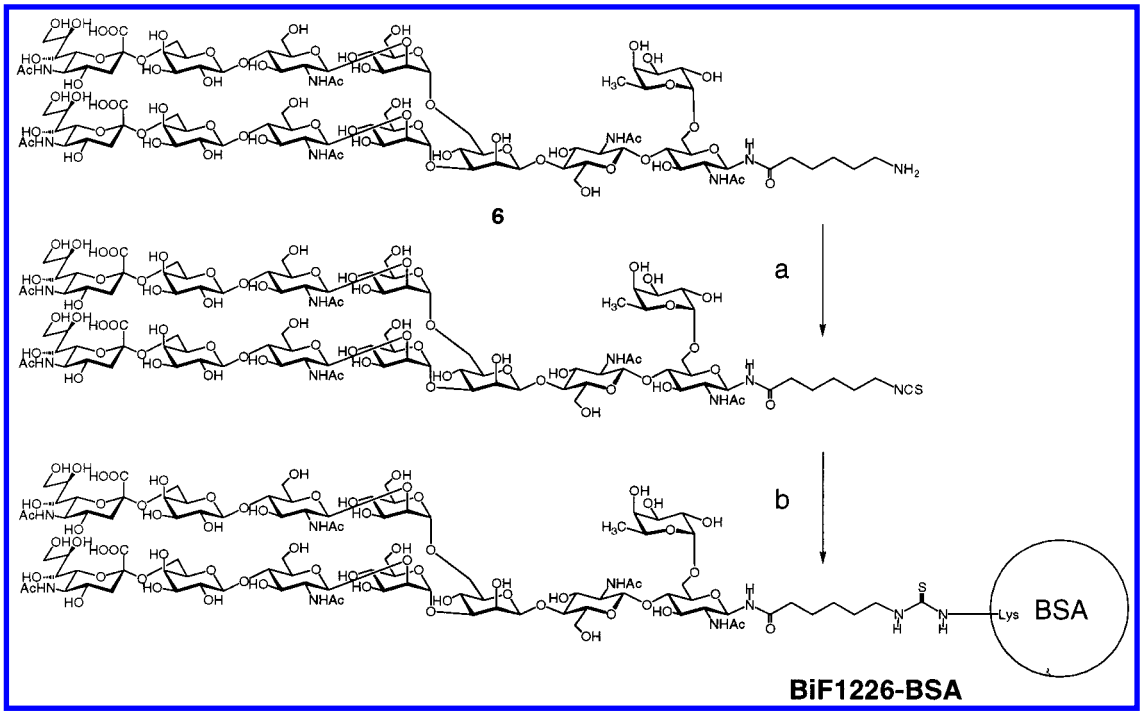

Figure 3. Activation of the amino group of the spacer at the reducing end of the synthetic *N*-glycans represented by dodecasaccharide **6** and the coupling to bovine serum albumin: (a) thiophosgene, $CH_2Cl_2-H_2O$, $NaHCO_3$, pH 8.5 (quantitative); (b) BSA, H_2O, $NaHCO_3$, pH 9.0.

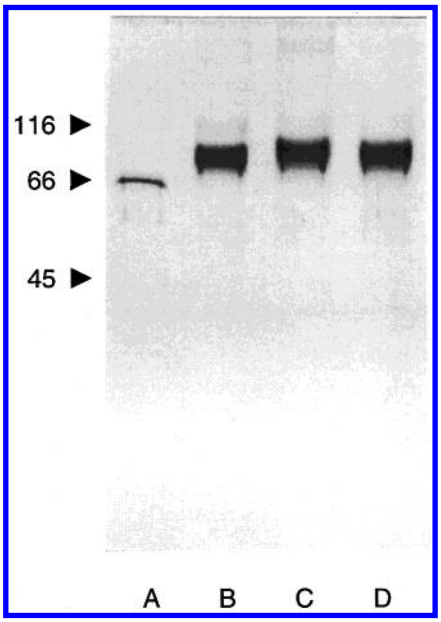

Figure 4. Visualization of the gel electrophoretic mobility under denaturing conditions of sugar-free BSA (A) and the neoglycoproteins with the core-fucosylated biantennary *N*-glycan **5** (B) and the α2,3-sialylated (C) and α2,6-sialylated (D) derivatives. Positions of marker proteins for molecular mass designation are indicated by arrowheads.

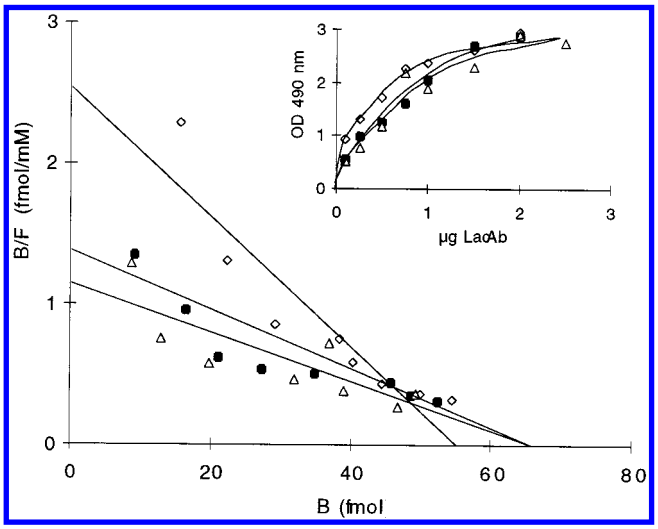

Figure 5. Scatchard plot analysis of the binding of biotinylated *β*-galactoside-binding immunoglobulin G fraction from human serum to surface-immobilized neoglycoproteins (◇, BiF10-BSA; ●, BiF1223-BSA; △, BiF1226-BSA) based on the extent of specific binding (inset) in one experimental series (for $x \pm$ SD, see Table 1).

albumin. The results of the colorimetric carbohydrate assay were reflected in the gel electrophoretic mobilities of the neoglycoproteins with shifts to increased molecular mass after chemical glycosylation (Figure 4). Starting from a pure synthetic compound, a set of core-fucosylated neoglycoproteins was prepared, thus eliminating microheterogeneity in the sugar part. The BSA conjugates were used to determine the recognition of the glycan chains by receptors in biochemical, cell biological, and histopathological assays. With these tools, binding properties to purified sugar receptors, cells, and organs can be unequivocally attributed to a defined carbohydrate structure. This approach overcomes the requirement for gauging individual contributions of various glycoforms. In a solid-phase assay the saturable and carbohydrate-dependent binding of three phylogenetically unrelated galactoside-specific proteins was determined. A representative scatchard plot is shown in Figure 5. The K_D and B_{max} data calculated from the solid-phase assays are compiled in Table 1. Since the fucose moiety was not directly involved in the recognition process of these galactose-specific probes, changes in the dissociation constants for core-fucosylated (BiF)

Table 1. Determination of the Apparent Dissociation Constant (K_D) for the Interaction of (Neo)glycoproteins with Sugar Receptors and the Number of Bound Probe Molecules at Saturation for *Viscum album* Agglutinin (VAA), Bovine Galectin-1, and the Human β-Galactoside-Binding Immunoglobulin G Subfraction (IgG) in a Solid-Phase Assay

	VAA		galectin-1		IgG	
matrix	K_D [a]	B_{max} [a]	K_D [a]	B_{max} [a]	K_D [a]	B_{max} [a]
BiF10-BSA (0.5 μg)	112.5 ± 56.2	(2.10 ± 0.10) × 10^{10}	377.1 ± 140	(2.04 ± 0.55) × 10^{10}	22.4 ± 0.79	(2.41 ± 1.23) × 10^{10}
BiF1223-BSA (0.5 μg)	511.5 ± 315	(1.32 ± 0.88) × 10^{10}	412.1 ± 223	(1.11 ± 0.14) × 10^{10}	45.8 ± 15.0	(2.68 ± 1.29) × 10^{10}
BiF12260BSA (0.5 μg)[b]	45.2 ± 35.0	(3.72 ± 1.95) × 10^{10}	1068 ± 113	(2.09 ± 0.74) × 10^{10}	45.8 ± 26.1	(2.78 ± 1.14) × 10^{10}
Bi9-BSA (0.5 μg)[e]	26.7 ± 11.6	(4.6 ± 1.9) × 10^{10}	900.1 ± 176	(42.8 ± 12.5) × 10^{10}	32.9 ± 19.6	(0.35 ± 0.1) × 10^{10}
Bi1123-BSA (0.5 μg)[e]	938.4 ± 661	(8.2 ± 4.4) × 10^{10}	829.5 ± 501	(42.0 ± 16.5) × 10^{10}	87.3 ± 62.7	(0.38 ± 0.1) × 10^{10}
Bi1126-BSA (0.5 μg)[e]	8.7 ± 4.5	(6.1 ± 1.4) × 10^{10}	1025.5 ± 619	(48.7 ± 18.4) × 10^{10}	33.9 ± 4.6	(0.46 ± 0.1) × 10^{10}
Lac-BSA (diazo) (3 μg)[c,e]	312.4 ± 190	(4.7 ± 2.3) × 10^{10}	1127.2 ± 53.3	(34.6 ± 17.6) × 10^{10}	139.0 ± 87.6	(0.70 ± 0.1) × 10^{10}
Lac-BSA (thio) (0.5 μg)[c,e]	13.4 ± 7.3	(5.1 ± 0.2) × 10^{10}	516.0 ± 20.3	(83.3 ± 6.5) × 10^{10}	7.6 ± 5.2	(0.65 ± 0.1) × 10^{10}
ASF (1 μg)[d,e]	7.4 ± 2.6	(4.9 ± 0.5) × 10^{10}	819.0 ± 268	(37.5 ± 10.7) × 10^{10}	69.2 ± 40.2	(0.43 ± 0.1) × 10^{10}

[a] K_D is given in nM. B_{max} is expressed as the number of bound probe molecules per well. [b] The assays with VAA and the neoglycoprotein BiF1226-BSA were performed with 0.25 μg as matrix. [c] Bovine serum albumin (BSA) was glycosylated by covalent attachment of either the diazophenyl derivative (diazo) or the *p*-isothiocyanatophenyl derivative (thio) of *p*-aminophenyl β-D-lactoside. [d] Asialofetuin. Each value is given as the mean ± SD from at least four independent experimental series, the quantity of (neo)glycoprotein for coating in μg/well being given for each type of substance. [e] From ref 12.

and unsubstituted (Bi) biantennary *N*-glycans can mainly be attributed to changes in the orientation of the α1,6-arm.[16−19] Aside from mastering the initial synthetic task, the availability of this set of neoglycoproteins facilitates quantification of the impact of *N*-glycan outer chain topology on protein−carbohydrate interactions. The dissociation constant K_D of homodimeric cross-linking galectin-1 was lowered by a factor of about 2 for the conjugates of decasaccharide **5** (BiF10-BSA) and the α2,3-sialylated dodecasaccharide **7** (BiF1223-BSA), relative to their counterparts lacking core fucosylation (Table 1). These two BiF-BSA neoglycoproteins also surpassed the ligand qualities of the natural glycoprotein asialofetuin, which is known to display predominantly triantennary *N*-glycans. Core-fucosylation-dependent increase of extended α1,6-arm conformers therefore appears to influence the affinity for galectin-1 more favorably than additional *N*-glycan branching, a crucial factor for the trimeric asialoglycoprotein receptor.[6,7]

Conversely, the trefoil-structure-forming mistletoe lectin (VAA), with two binding sites per galactoside-binding B-chain in the $[AB]_2$ tetramer,[36,37] did not benefit from core fucosylation. Noticeably, the relative affinity decreased about 5-fold for the decasaccharide **5** (BiF10-BSA) and its α2,6-sialylated derivative **6** (BiF1226-BSA) (Table 1). The relative affinity to this lectin was enhanced for high-density displays of lactose (Lac-BSA (thio)) or multibranched *N*-glycans present in ASF. Depending on the lectin, topological changes of the carbohydrate ligand can lead to adverse changes of affinity, a result so far not experimentally documented for core-fucosylated chains using this assay. Relative to the two lectins, the binding affinity of the immunoglobulin G fraction from human serum was less sensitive to the presence of a core fucose moiety (Table 1).

With regard to these results, the documented biological effects of core fucosylation[20−23] can be interpreted in a novel context. Besides direct recognition of the core fucose moiety, the influence of this modification on the glycan's topology also deserves to be taken into account, as shown by lectin binding in the solid-phase system.

To further investigate the impact of core fucosylation on the glycan's ligand properties, we compared carbohydrate-dependent binding of six neoglycoproteins (Figure 1) to native cells. Because of the very similar ligand densities of the neoglycoproteins, the results can be compared directly. Relative to purified lectins, the natural display of sugar-binding proteins found on tumor cell lines affords a model with increased complexity. The neoglycoproteins were labeled and used as markers in flow cytofluorometry under identical conditions to assess the percentage of positive cells and the median fluorescence intensity of carbohydrate-dependent binding. Thoroughly characterized leukemia/lymphoma, carcinoma, and melanoma cell lines were chosen as models relevant for drug targeting. Carcinoma cell lines included common tumor types such as breast, colon, lung, and ovarian tumors. Special care was exercised in the preparation of the cell material. To exclude any shift in binding-site expression during prolonged culture periods or by changes in the culture medium, aliquots of the cell batches were subjected to cytofluorometric monitoring on the same day in the absence or presence of the synthetic neoglycoproteins. Changes of fucose binding had been found for mouse L1210 leukemia and human Croco II B-lymphoblastoid cells.[38,39] Table 2 shows the complete set of data for the panel of nine (neo)-glycoproteins. Carbohydrate-specific binding was dependent on the histogenetic origin of the tumor cells and the state of cellular differentiation. The latter factor was exemplified by the pre-B and B-lymphoblastoid lines (BLIN-1, Croco II) with marked differences of the measured parameters. Especially for tumor lines of B- or T-cell origin, the influence of core fucosylation was very pronounced. Relatively, the effects exerted by the different terminal residues were significantly lower within a series of neoglycoproteins (Bi or BiF series). In addition, the positivity of the core-fucosylated glycans with leukemic lines such as KG-1 and the mammary adenocarcinoma line DU4475 was relatively strong when compared to cell labeling by fucose-free chains. This suggests that the orientation of the α1,6-arm can have a significant bearing on cell-binding properties. When candidates for targeting to epidermoid carcinoma cells of the lung are considered, the two core-fucosylated conjugates BiF10-BSA and BiF1223-BSA but not BiF1226-BSA will hit most of the cells, while the number of positive cells for the three tested colon adenocarcinoma lines reaches more than 50% only for Bi1126-BSA. Since the inhibition was invariably performed with a mixture of lactose and asialofetuin, a

Table 2. Flow Cytofluorometric Analysis of Binding of Neoglycoproteins with the Core-Fucosylated Biantennary *N*-Glycan (BiF10-BSA) and Its α2,3/α2,6-Sialylated Derivatives (BiF1223-BSA, BiF1226-BSA) and of Lactosylated Neoglycoproteins[a] and Asialofetuin (ASF) to Human Tumor Cell Lines of Diverse Histogenetic Origin[b]

	BiF10−BSA		BiF1223−BSA		BiF1226−BSA	
type of cell line	median fluorescence[b]	% of positive cells	median fluorescence[b]	% of positive cells	median fluorescence[b]	% of positive cells
BLIN-1	9.2	79.9	8.1	81.0	10.0	82.9
Croco II	46.5	33.7	40.5	34.7	40.6	36.5
CCRF-CEM	160.5	67.9	118.8	66.2	162.0	62.6
K-562	5.9	13.9	6.7	17.9	7.0	21.5
KG-1	30.4	78.0	26.7	76.0	24.3	75.9
HL-60	13.4	30.1	8.7	31.8	11.6	23.5
DU4475	42.1	43.1	41.1	47.8	45.9	48.3
NIH:OVCAR-3	15.7	23.8	13.8	21.1	17.6	37.0
C205	10.8	28.2	6.0	25.8	7.0	28.2
SW480	7.3	28.5	6.2	27.5	4.0	30.0
SW620	11.2	38.7	5.8	37.5	6.4	37.6
Hs-294T	7.0	20.1	3.7	16.5	3.7	16.3
HS-24	7.4	85.6	3.7	86.7	3.3	14.5
	Bi9−BSA[c]		Bi1123−BSA[c]		Bi1126−BSA[c]	
type of cell line	median fluorescence[b]	% of positive cells	median fluorescence[b]	% of positive cells	median fluorescence[b]	% of positive cells
BLIN-1	53.4	72.2	45.8	81.5	46.5	85.3
Croco II	17.4	10.6	26.3	24.5	21.5	24.8
CCRF-CEM	54.0	31.2	45.5	65.4	45.7	74.3
K-562	3.9	5.9	4.1	7.4	2.2	8.9
KG-1	16.8	13.5	26.0	35.7	18.4	29.3
HL-60	17.4	17.0	10.4	26.3	25.5	28.1
DU4475	5.3	6.9	9.4	13.7	5.2	8.6
NIH:OVCAR-3	*d*	*d*	*d*	*d*	*d*	*d*
C205	9.1	7.9	5.4	13.1	4.1	58.3
SW480	8.9	21.5	13.2	48.0	8.4	53.2
SW620	19.7	24.3	18.4	62.1	13.4	58.3
Hs-294T	4.3	8.7	4.3	9.4	5.6	10.5
HS-24	13.9	12.5	16.4	10.3	17.7	9.8
	LacBSA(Diazo)		LacBSA(Thio)		ASF	
type of cell line	median fluorescence[b]	% of positive cells	median fluorescence[b]	% of positive cells	median fluorescence[b]	% of positive cells
BLIN-1	1.6	11.4	18.1	71.3	16.7	82.3
Croco II	6.9	12.6	184.3	40.1	52.3	49.2
CCRF-CEM	10.2	21.6	553.8	66.5	140.9	53.8
K-562	0.2	5.5	27.8	40.6	8.2	12.8
KG-1	4.3	42.7	44.7	71.5	45.7	81.3
HL-60	5.1	10.3	68.2	22.9	12.6	14.4
DU4475	15.9	23.8	336.0	71.4	72.7	53.0
NIH:OVCAR-3	3.9	13.0	43.5	22.8	52.5	25.7
C205	0.2	6.5	18.0	29.7	10.7	25.9
SW480	1.1	8.4	8.2	43.5	7.8	41.9
SW620	1.4	9.3	9.8	35.2	9.8	38.5
Hs-294T	1.8	12.9	43.7	30.7	13.0	25.2
HS-24	3.4	13.3	45.1	31.9	22.9	25.6

[a] BSA was glycosylated by chemical attachment of either the diazophenyl (diazo) or the *p*-isothiocyanatophenyl derivative of *p*-aminophenyl *β*-D-lactoside. [b] The median fluorescence of binding of the fluorescent probe is given as extent of carbohydrate ligand-dependent binding by subtracting nonspecific binding from total binding for each cell line. [c] Eight individual examples from these data sets were illustrated by plots in ref 12. [d] Not determined.

participation of the fucose residue as a ligand in the galactose-sensitive reactions is unlikely.

Having shown that the neoglycoproteins interact via their *N*-glycans with binding sites on tumor cell surfaces in vitro, we next addressed the question of whether these markers can also be applied in histopathology. Routinely fixed sections of various types of lung cancer were analyzed. The binding pattern revealed nonuniform characteristics; in particular, large-cell carcinomas and carcinoids reacted differently with the decasaccharide (BiF10-BSA) and each of the two sialylated BiF derivatives (Figure 6). The fact that a monoclonal antibody, recognizing the core fucosyl determinant of *N*-glycans,[25] was bound to at least 44.4% of the tested cases underscores that the occurrence of this modification is a frequent event in human tumor biology (Figure 6). In comparison to the fucose-free nona- and undecasaccharide neoglycoproteins (Bi-BSA series), the α2,3-sialylated dodecasaccharide (BiF1223-BSA) was positive in a higher percentage of cases (Figures 6 and 7). This adds more evidence for an impact of core fucosylation on the binding properties of *N*-glycans, as already indicated by the solid-phase and flow cytofluorometric assays. For neoglycoproteins terminating with galactose, the examined cases of adenocarcinoma were more reactive toward the core-fucosylated decasaccharide (BiF10-BSA) (Figure 7). An even more pronounced difference was found for epidermoid carcinoma, which

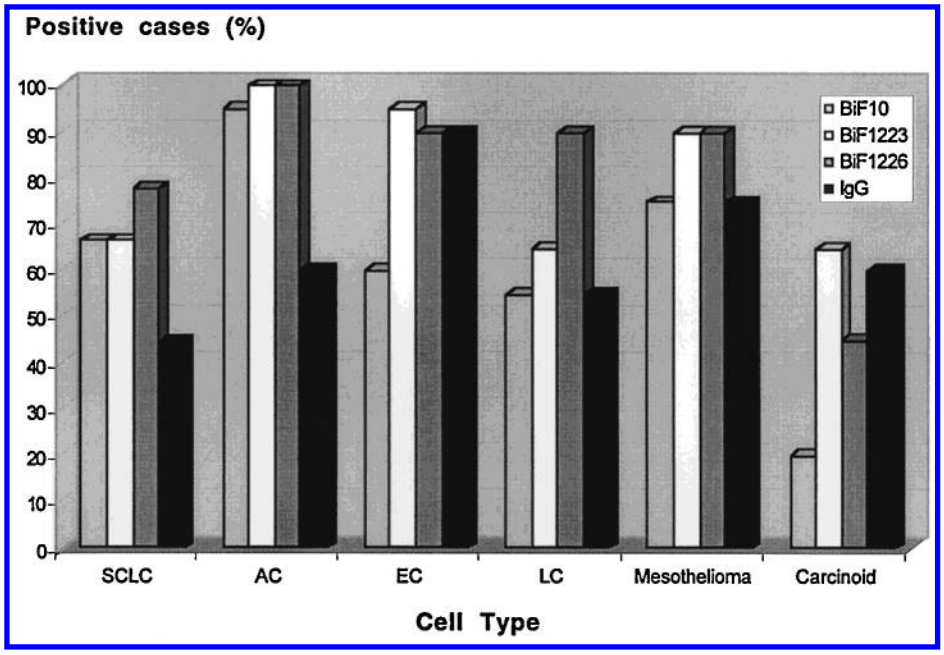

Figure 6. Quantitative evaluation of the percentage of positive cases for sections of small-cell anaplastic lung carcinoma (SCLC; $N = 18$), non-small-cell lung carcinoma ($N = 60$), i.e., adenocarcinoma (AC; $N = 20$), epidermoid carcinoma (EC, $N = 20$), large-cell carcinoma (LC; $N = 20$), mesothelioma ($N = 20$), and carcinoid ($N = 20$), grouped for the three types of labeled neoglycoproteins (BiF10-BSA, BiF1223-BSA, BiF1226-BSA), and the monoclonal antibody (IgG) with specificity to core fucosylation.

were recognized preferentially by the α2,6-sialylated dodecasaccharide (BiF1226-BSA).

To evaluate the potential of *N*-glycan-bearing glycoproteins as carriers of drugs to organs or distinct cell types,[9,40,41] we also monitored the pharmacokinetics of the radioiodinated neglycoproteins after injection into mice. The question to be answered was whether core fucosylation of the biantennary glycans will also be effective on this experimental level. The measurements of neoglycoprotein distribution in vivo revealed that the type of sialylation was influencing clearance (Table 3). The α2,6-sialylated dodecasaccharide (BiF1226-BSA) showed a considerably faster serum clearance than the α2,3-sialylated conjugate. This effect was not found for neoglycoproteins carrying nonfucosylated *N*-glycans.[12] Notably, the stability of the *N*-glycans in mouse serum over the assay period excluded a preferential desialylation. This result supports the notion that glycan microheterogeneity can account for multiphasic clearance from circulation, as shown for cholinesterases carrying biantennary complex *N*-glycans in mice.[42] Our data provide evidence that core fucosylation of a biantennary α2,6-sialylated *N*-glycan significantly accelerates neoglycoprotein clearance from the bloodstream. For the related undecasaccharide (Bi1126-BSA), 22.9% (after 1 h) and 13.95% (after 6 h) of the injected dose were found in circulation under identical experimental conditions.[12] Similar to the behavior of tyrosine-modified oligosaccharides isolated from bovine fetuin and porcine fibrinogen,[43,44] the uptake of the neoglycoproteins into organs other than liver, kidney, and spleen was rather low. In kidney a slight preference for the uptake of the sialylated neoglycoproteins was found, favoring the α2,3-sialylated *N*-glycan over the α2,6-isomer (Table 3). Enhanced tissue concentrations were also seen for neoglycointerleukin-1α carrying a spacer-bound derivative of *N*-acetylneuraminic acid.[45] Hence, sialylation may not generally lead to a prolonged circulatory half-life of *N*-glycan-exposing neoglycoproteins in mice. When considering means to increase serum half-life besides polysialic acids,[46] α2,3-sialylation appears to be superior to the α2,6-form in this context.

Conclusion

Reflecting the advances in carbohydrate chemistry and mechanistic understanding of protein−carbohydrate interactions, the emphasis in analyzing sugar recognition has shifted from elucidating sequences to designing the suitably shaped ligands. By extending the previously devised chemoenzymatic route to biantennary complex *N*-glycans, we herein describe the preparation of neoglycoproteins carrying homogeneous *N*-glycans with a core-fucosyl substitution. The application of these new markers in various test systems suggested that an altered orientation profile of the glycan's α1,6-arm was affecting overall performance. In assays with purified sugar receptors, structure-based conformational changes were shown to affect dissociation constants. In cell biological assays with tumor cell lines, cell-type- and differentiation-dependent results were documented. For lung cancer the reaction of tumor subtypes is shown using the glycan chains of neoglycoproteins as diagnostic agents. Monitoring the biodistribution of labeled neoglycoproteins revealed new approaches to prolong or shorten circulatory residence by core fucosylation. The presented approach to introduce distinct changes in the complex-type glycan part (here by core fucosylation) allows us to thoroughly examine the effects of a structural alteration, which is not directly involved in the set of immediate binding interactions. With the increasing emergence of glycans in biopharmaceuticals, the tailoring of their properties is desirable. Systematic evaluation of carbohydrate-dependent effects is essential to define an optimal composition for glycans that are part of a medicinal neoglycoprotein. It is noteworthy that the outlined chemoenzymatic strategy will allow us to

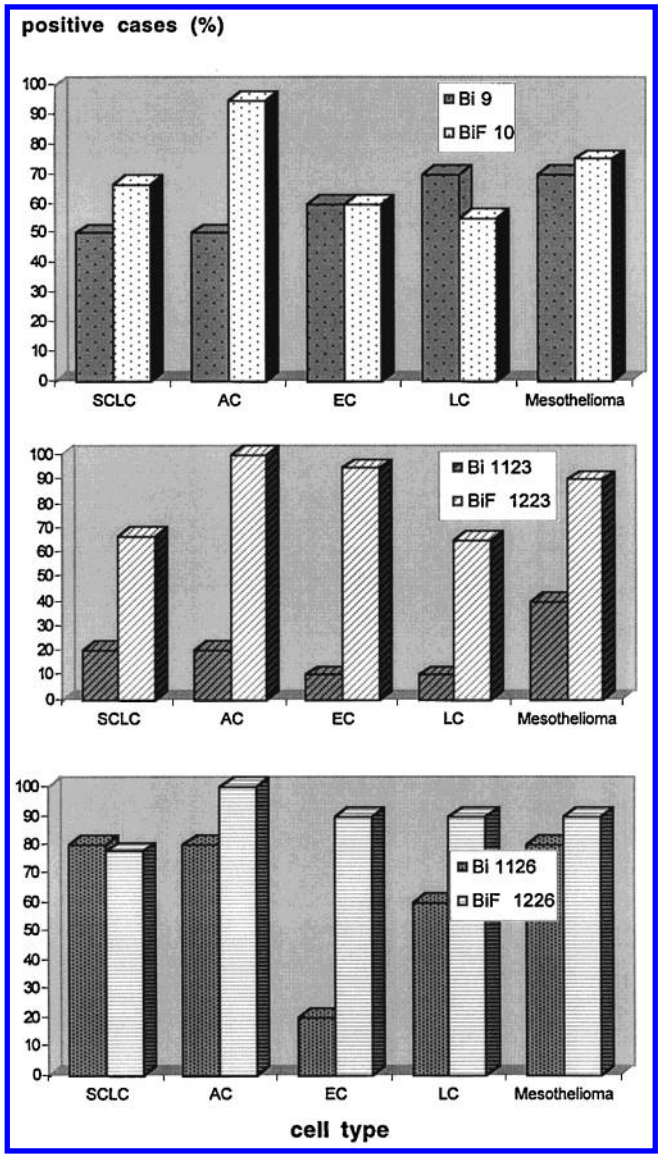

Figure 7. Quantitative evaluation of the percentage of positive cases for sections of small-cell lung cancer (SCLC), the three types of non-small lung cancer (for abbreviations, see legend to Figure 6), and mesothelioma when staining of tumor cells was compared after application of the three core-fucosylated *N*-glycans (BiF10-BSA, BiF1223-BSA, BiF1226-BSA) and their fucose-free counterparts (Bi9-BSA, Bi1123-BSA, Bi1126-BSA).

introduce substitutions not available from natural sources to broaden the scope of rational glycan modeling.

Experimental Procedures

General. NMR spectra were recorded with a Bruker AMX 500 spectrometer. HPLC separations were performed on a Pharmacia LKB gradient system 2249 equipped with a Pharmacia LKB detector VWM 2141 (Freiburg, Germany). For size exclusion chromatography a Pharmacia Hi Load Superdex 30 column (600 mm × 16 mm) was used, RP-HPLC was performed on a Macherey-Nagel Nucleogel RP 100-10 column (300 mm × 25 mm). Bovine serum albumin, β1,4-galactosyltransferase, α2,6-sialyltransferase, and nucleotide sugars were purchased from Sigma (Munich, Germany), and alkaline phosphatase (calf intestine, molecular biology grade) was purchased from Boehringer Mannheim (Germany). ESI mass spectra were recorded on a Finnigan TSQ 700 in methanol/water. MALDI-TOF mass spectra were collected by Dr. D. Renauer at the Boehringer Mannheim research facility (Tutzing, Germany) on a Voyager Biospectrometry workstation (Vestec/Perseptive) MALDI-TOF mass spectrometer, using 2,5-dihydroxybenzoic acid (DHB) as a matrix. We are grateful to Prof. J. C. Paulson (Cytel Corp., San Diego, CA) for a sample of recombinant α2,3-sialyltransferase.

The structures of the synthetic *N*-glycans were confirmed by the following 2D-NMR experiments: TOCSY, NOESY, HMQC, HMQC−COSY, HMQC distortionless enhancement by polarization transfer (DEPT), and HMQC−TOCSY. NMR specta were assigned according to the convention shown in Chart 1.

The schematic outline for the derivatization of the synthetic octasaccharide azide, prepared previously,[30] including spacer and terminal amino group introduction, is given in Figure 2.

***N*¹-(6-Benzyloxycarbonyl-6-aminohexanoylamido)-*O*-2-acetamido-2-deoxy-β-D-glucopyranosyl-(1→2)-*O*-α-D-mannopyranosyl-(1→3)-*O*-[2-acetamido-2-deoxy-β-D-glucopyranosyl-(1→2)-*O*-α-D-mannopyranosyl-(1→6)]-*O*-β-D-mannopyranosyl-(1→4)-*O*-(2-acetamido-3,6-di-*O*-benzyl-2-deoxy-β-D-glucopyranosyl)-(1→4)-*O*-[α-L-fucopyranosyl-(1→6)]-2-acetamido-3-*O*-benzyl-2-deoxy-β-D-glucopyranoside 3 (Bzl_3-BiF8AH-Z).** To a portion of 62.8 mg (35.7 μmol) of glycosyl azide **1** dissolved in 2.1 mL of absolute methanol were added 70 μL of triethylamine. The flask was flushed with argon followed by addition of 210 μL of propane-1,3-dithiol. After completion of the reaction (3.5 h, R_f(amine) = 0.13; TLC, 2-propanol/1 M NH_4OAc, 4:1) the solution was evaporated and dried in high vacuum for 15 min. The remainder was reacted with a solution of activated *Z*-aminohexanoic acid **2** prepared as follows. A total of 236 mg (0.89 mmol, 20 equiv) of *Z*-aminohexanoic acid **2** was dissolved in 3.5 mL of *N*-methylpyrrolidone. Subsequently, 136.3 mg (0.89 mmol, 20 equiv) of *N*-hydroxybenzotriazol, 285.8 mg (0.89 mmol, 20 equiv) of TBTU ((1*H*-benzotriazol-1-yl)-1,1,3,3-tetramethyluronium tetrafluoroborate), and 233 μL (1.32 mmol) of diisopropylethylamine were added. The mixture was stirred until a clear solution was obtained and was adjusted to pH 9.0 by adding 130 μL of diisopropylethylamine.

The dried glycosylamine was dissolved in 2.50 mL of the solution prepared as above, and the pH was adjusted to 9.0 with diisopropylethylamine. After 30 min at ambient temperature (TLC, 2-propanol/1 M NH_4OAc, 4:1), 0.5 mL of the solution was added and stirring was continued for 5 min. The reaction mixture was evaporated and dried in high vacuum. Purification of the remainder was performed by RP-HPLC (acetonitrile/water, gradient of 35−45% CH_3CN in 40 min; flow rate = 8 mL/min, Macherey-Nagel Nucleogel RP 100−10 (300 mm × 25 mm)).

Yield: 36.8 mg (52.0%). R_f(amine) = 0.13 (2-propanol/1 M NH_4OAc, 4:1). R_f(**3**) = 0.34 (2-propanol/1 M NH_4OAc, 4:1). $[\alpha]^{22}_D$ −10.8° (*c* 0.5, CH_3CN/H_2O, 1:1). $C_{91}H_{130}N_6O_{42}$ (M = 1980.05). ESI-MS: M_{calcd} = 1978.84, M_{found} = 990.7 $(M + 2H)^{2+}$.

^{1}H NMR (500 MHz, D_2O/CD_3CN = 9:1): δ = 7.29−7.06 (m, 20H, Ar), 4.89 (bs, 2H, OCH_2), 4.86 (d, $J_{1,2}$ < 1.0 Hz, 1H, H-1^4), 4.77 (d, J_{gem} = 11.8 Hz, 1H, OCH_2), 4.75 (d, $J_{1,2}$ = 8.8 Hz, 1H, H-1^1), 4.73 (d, J_{gem} = 12.1 Hz, 1H, OCH_2), 4.63 (d, $J_{1,2}$ = 3.6 Hz, 1H, H-1^8), 4.56 (d, $J_{1,2}$ < 1.0 Hz, 1H, H-1$^{4'}$), 4.49 (d, $J_{1,2}$ = 8.2 Hz, 1H, H-1^2), 4.48 (d, J_{gem} = 11.8 Hz, 1H, OCH_2), 4.47 (d, $J_{1,2}$ < 1.0 Hz, 1H, H-1^3), 4.42 (d, J_{gem} = 12.0 Hz, 1H, OCH_2), 4.32 (d, $J_{1,2}$ = 8.4 Hz, 1H, H-1^5), 4.25 (2d, J_{gem} = 11.8 Hz, 2H, OCH_2), 4.08 (d, $J_{1,2}$ = 8.3 Hz, 1H, H-1$^{5'}$), 3.94 (dd, $J_{1,2}$ < 1.0 Hz, $J_{2,3}$ = 2.8 Hz, 1H, H-2^4), 3.88 (dd, $J_{1,2}$ < 1.0 Hz, $J_{2,3}$ = 2.9 Hz, 1H, H-2^3), 3.86 (dq, $J_{4,5}$ = 9.4 Hz, $J_{5,6}$ = 6.6 Hz, 1H, H-5^8), 3.76 (dd, $J_{4,5}$ = $J_{3,4}$ = 9.0 Hz, H-4^1, H-4^2), 3.38−3.19 (m, 12H, H-6b^2, H-5^1, H-6b^3, H-4^4, H-5$^{4'}$, H-3^3, H-3^5, H-4$^{4'}$, H-3$^{5'}$, H-4$^{5'}$, H-4^5, H-5^5), 3.72−3.40 (m, 27H, H-6a^3, H-2^2, H-3^4, H-6a^5, H-2^1, H-4^3, H-6a^4, H-6a^1, H-2$^{4'}$, H-6a$^{4'}$, H-3^8, H-2^8, H-6a^2, H-3$^{4'}$, H-3^2, H-5^4, H-6b^4, H-6b^5, H-6a$^{5'}$, H-6b$^{5'}$, H-2^5, H-4^8, H-3^1, H-6b$^{4'}$, H-6b^1, H-2$^{5'}$, H-5^2, H-6b^2), 3.05 (m, 1H, H-5^3), 2.97 (m, 1H, H-5$^{5'}$), 2.89 (t, J_{gem} = 6.6 Hz, 2H, ϵ-CH_2), 2.00 (t, J_{gem} = 7.1 Hz, 2H, α-CH_2), 1.82, 1.81, 1.69, 1.56 (4s, 12H, NAc), 1.34 (m,

Table 3. Biodistribution of ^{125}I-Neoglycoproteins (percent injected dose per gram of tissue) in Ehrlich Solid Tumor-Bearing Mice after 1 and 6 h[a]

	1 h			6 h		
tissues	BiF10-BSA	BiF1223-BSA	BiF1226-BSA	BiF10-BSA	BiF1223-BSA	BiF1226-BSA
Blood	3.11 ± 0.17	18.83 ± 0.75	7.36 ± 0.42	1.65 ± 0.20	9.41 ± 0.64	3.61 ± 0.28
Liver	2.86 ± 0.15	3.40 ± 0.09	5.43 ± 0.27	1.39 ± 0.10	1.96 ± 0.16	2.60 ± 0.12
Kidneys	2.41 ± 0.06	3.94 ± 0.20	3.05 ± 0.15	1.22 ± 0.08	2.74 ± 0.28	1.72 ± 0.10
Spleen	1.31 ± 0.14	3.04 ± 0.30	3.63 ± 0.32	0.63 ± 0.05	1.38 ± 0.19	1.45 ± 0.04
Heart	0.94 ± 0.09	2.73 ± 0.06	1.52 ± 0.17	0.42 ± 0.02	1.71 ± 0.19	0.78 ± 0.04
Lung	1.27 ± 0.07	2.28 ± 0.09	2.13 ± 0.23	0.77 ± 0.11	1.77 ± 0.26	1.18 ± 0.06
Thymus	1.29 ± 0.35	1.58 ± 0.12	1.20 ± 0.15	0.50 ± 0.07	1.11 ± 0.22	0.62 ± 0.04
Pancreas	1.14 ± 0.14	0.99 ± 0.06	0.98 ± 0.04	0.46 ± 0.04	0.77 ± 0.04	0.50 ± 0.02
Lymph node	0.84 ± 0.06	1.64 ± 0.10	0.97 ± 0.09	0.39 ± 0.02	1.15 ± 0.04	0.61 ± 0.06
Muscle	0.43 ± 0.02	0.36 ± 0.02	0.39 ± 0.02	0.18 ± 0.02	0.32 ± 0.08	0.22 ± 0.01
Vertebrae	0.70 ± 0.03	1.20 ± 0.07	1.04 ± 0.07	0.36 ± 0.02	0.77 ± 0.08	0.48 ± 0.01
Brain	0.13 ± 0.01	0.28 ± 0.02	0.17 ± 0.01	0.05 ± 0.01	0.17 ± 0.02	0.09 ± 0.01
Tumor	1.65 ± 0.06	3.89 ± 0.20	2.47 ± 0.14	0.90 ± 0.10	3.08 ± 0.47	1.36 ± 0.09

[a] Each value represents the mean ± SEM for four animals.

Chart 1

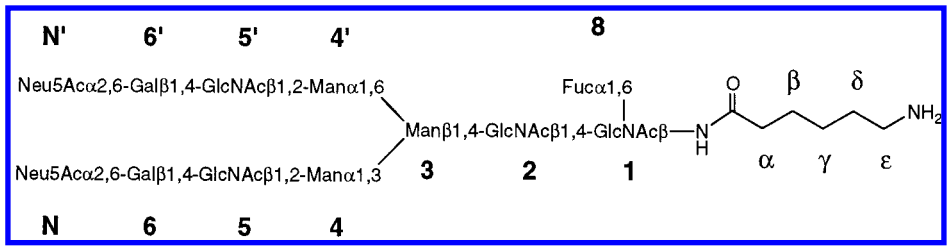

2H, β-CH_2), 1.27 (dt, 2H, $J_{\gamma,\delta} = J_{\delta,\epsilon} = 7.3$ Hz, 2H, δ-CH_2), 1.05 (dt, 2H, $J_{\gamma,\beta} = J_{\gamma,\delta} = 7.3$ Hz, 2H, γ-CH_2), 0.95 (d, $J_{5,6} = 6.6$ Hz, 3H, H-6^8).

^{13}C NMR (125 MHz, D_2O/CD_3CN = 9:1): δ = 169.91, 169.73, 169.32, 168.97 C=O, 156.34 C=O urethane, 138.79, 138.45, 137.93, 137.80 C-i Ar, 128.59, 128.03, 127.96, 127.84 Ar, 100.71 C-1^2, 100.38 C-1^3, 100.00 C-1^5, 99.79 C-1$^{5'}$, 99.65 C-1^4, 99.12 C-1^8, 96.77 C-1$^{4'}$, 81.13 C-3^1, 81.01 C-3^3, 80.68 C-3^2, 78.58 C-1^1, 77.22 C-4^2, 77.15 C-2^4, 76.88 C-2$^{4'}$, 76.16 C-4^1, 76.14 C-5^5, 75.90 C-5$^{5'}$, 74.63 C-5^3, 74.44 OCH_2, 74.32 C-5^2, 73.63 OCH_2, 73.58 C-5^4, 73.56 C-3^5, 73.48 C-3$^{5'}$, 73.23 OCH_2, 72.87 C-5$^{4'}$, 72.02 C-4^8, 70.58 C-2^3, 70.20 C-4^5, 69.92 C-3^8, C-3$^{4'}$, 69.82 C-4$^{5'}$, 69.79 C-3^4, 68.97 C-6$^{4'}$, 68.45 C-2^8, 67.41 C-4$^{4'}$, 67.39 C-4^4, 66.78 C-5^8, 66.64 C-6^4, 66.53 OCH_2, 65.59 C-4^3, 66.57 C-6^3, 61.74 C-6^1, 61.70 C-6^2, 61.02 C-6^5, 60.61 C-6$^{5'}$, 55.68 C-2$^{5'}$, C-2^5, 55.08 C-2^2, 53.43 C2^1, 40.71 C-6 AH, 35.99 C-2 AH, 29.25 C-5 AH, 25.91 C-4 AH, 25.28 C-3 AH, 22.90, 22.68, 22.44 NAc, 16.08 C-6^8.

***N*^{1}-(6-Aminohexanoylamido)-*O*-2-acetamido-2-deoxy-β-D-glucopyranosyl-(1→2)-*O*-α-D-mannopyranosyl-(1→3)-*O*-[2-acetamido-2-deoxy-β-D-glucopyranosyl-(1→2)-*O*-α-D-mannopyranosyl-(1→6)]-*O*-β-D-mannopyranosyl-(1→4)-2-acetamido-2-deoxy-β-D-glucopyranosyl-(1→4)-*O*-[α-L-fucopyranosyl-(1→6)]-2-acetamido-2-deoxy-β-D-glucopyranoside 4 (BiF8AH).** A 32 mg (16.2 μmol) portion of the protected octasaccharide **3** was dissolved in a mixture of 6.7 mL of methanol and 330 μL of acetic acid. After addition of 61 mg of palladium(II) oxide hydrate (84.6% Pd), the suspension was stirred under hydrogen at atmospheric pressure for 24 h (TLC, 2-propanol/1 M NH_4OAc, 2:1). The catalyst was removed by centrifugation and washed three times with 10% acetic acid in methanol. The combined supernatants were concentrated, and the remainder (27.5 mg) was purified by gel filtration (column, Pharmacia Hi Load Superdex 30, 600 mm × 16 mm; mobile phase, 100 mM NH_4HCO_3; flow rate, 750 μL/min; detection, 220 and 260 nm) and lyophilized.

Yield: 23.4 mg (92.0%). R_f = 0.29 (2-propanol/1 M NH_4OAc, 2:1). $[\alpha]^{22}_D = -21.8°$ (*c* 0.31, H_2O). $C_{62}H_{106}N_6O_{40}$ (*M* = 1575.54). ESI-MS: M_{calcd} = 1574.64, M_{found} = 1575.1 $(M)^+$.

^{1}H NMR (500 MHz, D_2O/CD_3CN = 9:1): δ = 4.93 (d, $J_{1,2}$ < 1.0 Hz, 1H, H-1$^4\alpha$), 4.85 (d, $J_{1,2}$ = 9.8 Hz, 1H, H-1$^1\beta$), 4.73 (d, $J_{1,2}$ < 1.0 Hz, 1H, H-1$^{4'}\alpha$), 4.69 (d, $J_{1,2}$ = 3.7 Hz, 1H, H-1^8), 4.57 (d, $J_{1,2}$ < 1.0 Hz, 1H, H-1^3), 4.49 (d, $J_{1,2}$ = 9.2 Hz, 1H, H-1^2), 4.37 (d, $J_{1,2}$ = 8.4 Hz, 2H, H-1^5, H-1$^{5'}$), 4.05 (dd, $J_{2,3}$ = 2.6 Hz, 1H, H-2^3), 3.99 (dd, $J_{2,3}$ = 2.9 Hz, 1H, H-2^4), 3.94 (dq, $J_{4,5}$ = 9.4 Hz, $J_{5,6}$ = 6.6 Hz, 1H, H-5^8), 3.90 (dd, $J_{2,3}$ = 2.9 Hz, 1H, H-2$^{4'}$), 3.75−3.24 (m, 41H, H-6a^3, H-6a^5, H-6a$^{5'}$, H-6a^4, H-6a$^{4'}$, H-3^4, H-3$^{4'}$, H-6a^1, H-6a^2, H-3^8, H-2^1, H-2^2, H-4^8, H-6b^3, H-2^8, H-4^8, H-3^3, H-6b^5, H-6b$^{5'}$, H-6b^2, H-5^4, H-3^1, H-3^2, H-4^1, H-4^2, H-6b^1, H-2$^{5'}$, H-2^5, H-5^1, H-6b^4, H-6b$^{4'}$, H-5^2, H-5^3, H-5$^{4'}$, H-3^5, H-3$^{5'}$, H-4^4, H-4$^{4'}$, H-4^5, H-4$^{5'}$, H-5^5, H-5$^{5'}$), 2.79 (t, $J_{\delta,\epsilon}$ = 7.8 Hz, 2H, ϵ-CH_2), 2.09 (t, $J_{\alpha,\beta}$ = 7.3 Hz, 2H, α-CH_2), 1.82, 1.81, 1.69, 1.56 (4s, 12H, NAc), 1.47 (m, 2H, β-CH_2), 1.27 (m, 2H, δ-CH_2), 1.14 (m, 2H, γ-CH_2), 1.01 (d, $J_{5,6}$ = 6.6 Hz, 3H, H-6^8).

^{13}C NMR (125 MHz, D_2O/CD_3CN = 9:1): δ =178.0, 175.5, 175.4, 175.3 C=O, 101.88 C-1^2, 101.27 C-1^3, 100.49 C-1^5, C-1$^{5'}$, 100.39 C-1^4, 100.20 C-1^8, 97.86 C-1$^{4'}$, 81.26 C-3^3, 80.52 C-4^2, 79.56 C-4^1, 79.19 C-1^1, 77.42 C-2^4, 77.28 C-2$^{4'}$, 76.70 C-5$^{5'}$, C-5^5, 76.01 C-5^1, 75.27 C-5^3, 75.20 C-5^2, 74.38 C-3^2, 74.24 C-3^5, 74.14 C-3$^{5'}$, 73.71 C-5$^{4'}$, 73.42 C-5^4, 72.91 C-3^1, C-5^4, 72.69 C-4^8, 71.01 C-2^3, 70.80 C-45′, C-4^5, 70.44 C-3^8, 70.32 C-3$^{4'}$, C-3^4, 69.01 C-2^8, 68.23 C-4$^{4'}$, 68.18 C-4^4, 67.59 C-6^1, C-5^8, 66.77 C-6^3, 66.61 C-4^3, 62.55 C-6$^{4'}$, 62.47 C-6^4, 61.53 C-6^5, C-6$^{5'}$, 60.89 C-6^2, 56.21 C-2^5, C-2$^{5'}$, 55.79 C-2^2, 54.69 C-2^1, 40.07 C-6 AH, 36.30 C-2 AH, 27.17 C-5 AH, 25.85 C-4 AH, 25.32 C-3 AH, 23.23, 22.90 NAc, 16.28 C-6^8.

***N*^{1}-(6-Aminohexanoylamido)-*O*-β-D-galactopyranosyl-(1→4)-*O*-2-acetamido-2-deoxy-β-D-glucopyranosyl-(1→2)-*O*-α-D-mannopyranosyl-(1→3)-*O*-[β-D-galactopyranosyl-(1→4)-*O*-2-acetamido-2-deoxy-β-D-glucopyranosyl-(1→2)-*O*-α-D-mannopyranosyl-(1→6)]-*O*-β-D-mannopyranosyl-(1→4)-*O*-2-acetamido-2-deoxy-β-D-glucopyranosyl-(1→4)-*O*-[α-L-fucopyranosyl-(1→6)]-2-acetamido-2-deoxy-β-D-glucopyranoside 5 (BiF10AH).** A 6.8 mg portion (4.32 μmol) of octasaccharide **4** was dissolved in 2.4 mL of a 20 mM sodium cacodylate buffer at pH 7.4. The buffer contained 1.7 mg of bovine serum albumin, 4.34 μmol of NaN_3, 2.43 μmol of $MnCl_2$, 8.3 mg (12.5 μmol) of uridine-5′-diphosphogalactose, 10.3 U of alkaline phosphatase (EC 3.1.3.) and 208 mU of GlcNAc-β1,4-galactosyltransferase (EC 2.4.1.22). The reaction mixture was incubated for 48 h at 37 °C. After complete reaction (TLC, 2-propanol/1 M NH_4OAc, 2:1) the precipitate was removed by centrifugation. The supernatant was concentrated to a volume of 450 μL, purified by gel filtration (column, Pharmacia Hi Load Superdex 30, 600 mm × 16 mm; mobile phase, 100 mM

NH_4HCO_3; flow rate, 750 μL/min; detection, 220 and 260 nm), and lyophilized.

Yield: 6.1 mg (75.0%). $R_f = 0.15$ (2-propanol/1 M NH_4OAc, 2:1). $[\alpha]^{22}_D = -2.2°$ (*c* 0.63, H_2O). $C_{74}H_{126}N_6O_{50}$ ($M = 1899.82$). ESI-MS: $M_{calcd} = 1898.76$, $M_{found} = 950.7$ $(M + 2H)^{2+}$.

^{1}H NMR (500 MHz, D_2O/CD_3CN, 9:1): $\delta = 4.90$ (d, $J_{1,2} < 1.0$ Hz, 1H, H-1^A), 4.85 (d, $J_{1,2} = 9.7$ Hz, 1H, H-1^1), 4.70 (d, $J_{1,2} < 1.0$ Hz, 1H, H-1$^{A'}$), 4.66 (d, $J_{1,2} = 3.2$ Hz, 1H, H-1^8), 4.56 (d, $J_{1,2} < 1.0$ Hz, 1H, H-1^3), 4.46 (d, $J_{1,2} = 8.1$ Hz, 1H, H-1^2), 4.36 (d, $J_{1,2} = 7.5$ Hz, 2H, H-1^5, H-1$^{5'}$), 4.25 (d, $J_{1,2} = 7.6$ Hz, 1H, H-1^6), 4.24 (d, $J_{1,2} = 7.6$ Hz, 1H, H-1^6), 4.03 (dd, $J_{2,3} < 1.5$ Hz, 1H, H-2^3), 3.97 (dd, $J_{2,3} < 1.5$ Hz, 1H, H-2^4), 3.91 (dq, $J_{4,5} = 13.3$ Hz, $J_{5,6} = 6.6$ Hz, 1H, H-5^8), 3.87 (dd, $J_{2,3} < 1.5$ Hz, 1H, H-2$^{4'}$), 3.80−3.63 (m, 15H, H-6a$^{5'}$, H-6a^5, H-6a^3, H-4^6, H-4$^{6'}$, H-6a^4, H-6a$^{4'}$, H-3^4, H-3$^{4'}$, H-6a^1, H-6a^2, H-3^8, H-6b$^{5'}$, H-6b^5, H-2^1), 3.63−3.44 (m, 27H, H-2^2, H-4^8, H-6b^3, H-2^8, H-6a^6, H-6a$^{6'}$, H-6b^6, H-6b$^{6'}$, H-6b^2, H-2^5, H-2$^{5'}$, H-6b^2, H-3^1, H-3^2, H-4^1, H-3^5, H-3$^{5'}$, H-4^5, H-4$^{5'}$, H-4^2, H-5^1, H-5^6, H-5$^{6'}$, H-6b^1, H-5^1, H-3^6, H-3$^{6'}$), 3.43−3.26 (m, 11H, H-6b^4, H-6b$^{4'}$, H-5^2, H-5^3, H-5$^{4'}$, H-5^5, H-5$^{5'}$, H-2^6, H-2$^{6'}$, H-4$^{4'}$, H-4^4), 2.73 (t, $J_{\delta,\epsilon} = 7.7$ Hz, 2H, ϵ-CH_2), 2.06 (t, $J_{\alpha,\beta} = 7.2$ Hz, 2H, α-CH_2), 1.87, 1.83, 1.82, 1.78 (4s, 12H, NAc), 1.43 (m, 2H, β-CH_2), 1.38 (m, 2H, δ-CH_2), 1.13 (m, 2H, γ-CH_2), 0.98 (d, $J_{5,6} = 6.6$ Hz, 3H, H-6^8).

^{13}C NMR (125 MHz, D_2O/CD_3CN, 9:1): $\delta = 175.5$, 175.4 C=O, 103.82 C-1^6, C-1$^{6'}$, 101.90 C-1^2, 101.32 C-1^3), 100.36 C-1^5, C-1$^{5'}$, 100.29 C1^8, 100.27 C-1^4, 97.89 C-1$^{A'}$1, 81.28 C-3^3, 80.49 C-4^2, 79.46 C-4^1, C-4^5, C-4$^{5'}$, 79.20 C-1^1, 77.35 C-2^4, 77.22 C-2$^{4'}$, 76. 22 C-3^5, C-3$^{5'}$, 76.08 C-5^1, 75.61 C-5^5, C-5$^{5'}$, 75.30 C-5^3, C-5$^{4'}$, 74.42 C-3^2, C-5^4, 73.74 C-5^2, 73.49 C-3^1, 73.41 C-3^6, C-3$^{6'}$, 72.94 C-5$^{6'}$, 72.82 C-5^6, 72.71 C-4^8, 71.84 C-2^6, C-2$^{6'}$, 71.04 C-2^3, 70.44 C-3^4, C-3$^{4'}$, 70.33 C-3^8, 69.41 C-4^6, C-4$^{6'}$, 69.01 C-2^8, 68.22 C-4^4, 68.18 C-4$^{4'}$, 67.66 C-5^8, C-6^1, 66.70 C-6^3, 66.59 C-4^3, 62.58 C-6$^{4'}$, 62.51 C-6^4, 61.87 C-6^6, C-6$^{6'}$, 60.89 C-6^2, C-6^5, C-6$^{5'}$, 55.83 C-2^2, 55.75 C-2^5, C-2$^{5'}$, 54.67 C-2^1, 40.16 C-6 AH, 36.33 C-2 AH, 27.63 C-5 AH, 25.90 C-4 AH, 25.39 C-3 AH, 23.23, 22.90 NAc, 16.30 C-6^8.

***N*^{1}-(6-Aminohexanoylamido)-*O*-(5-acetamido-3,5-dideoxy-α-D-glycero-D-galacto-2-nonulopyranulosonic acid)-(2→6)-*O*-β-D-galactopyranosyl-(1→4)-*O*-2-acetamido-2-deoxy-β-D-gluco-pyranosyl-(1→2)-*O*-α-D-mannopyranosyl-(1→3)-*O*-[(5-acetamido-3,5-dideoxy-α-D-glycero-D-galacto-2-nonulopyranulosonic acid)-(2→6)-*O*-β-D-galactopyranosyl-(1→4)-*O*-2-acetamido-2-deoxy-β-D-glucopyranosyl-(1→2)-*O*-α-D-mannopyranosyl-(1→6)]-*O*-β-D-mannopyranosyl-(1→4)-*O*-2-acetamido-2-deoxy-β-D-glucopyranosyl−(1→4)-*O*-[α-L-fucopyranosyl-(1→6)]-2-acetamido-2-deoxy-β-D-glucopyranoside 6 (BiF1226AH).** A 6.5 mg portion (4.12 μmol) of octasaccharide **4** was dissolved in 2.4 mL of a 20 mM sodium cacodylate buffer, pH 7.4. The buffer contained 1.7 mg of bovine serum albumin, 4.34 μmol of NaN_3, 2.43 μmol of $MnCl_2$, 8.3 mg (12.5 μmol) of uridine-5′-diphosphogalactose, 10.3 U of alkaline phosphatase (EC 3.1.3.), and 208 mU of GlcNAc-β1,4-galactosyltransferase (EC 2.4.1.22). The reaction mixture was incubated for 48 h at 37 °C. After complete reaction (TLC, 2-propanol/1 M NH_4OAc, 2:1), 7.0 mg (9.1 μmol) of cytidine-5′-monophospho-*N*-acetylneuraminic acid and 75 mU of β-galactoside-α2,6-sialyltransferase (EC 2.4.99.1) were added. After adjustment of the pH to 6.0, incubation at 37 °C was continued for 24 h. A second portion of 7.0 mg (9.1 μmol) of cytidine-5′-monophospho-*N*-acetylneuraminic acid and 75 mU of β-galactoside-α2,6-sialyltransferase were added (pH 6.0). Incubation at 37 °C for 16 h was followed by removal of the precipitate by centrifugation. The supernatant was concentrated to a volume of 450 μL, purified by gel filtration (column, Pharmacia Hi Load Superdex 30, 600 mm × 16 mm; mobile phase, 100 mM NH_4HCO_3; flow rate, 750 μL/min; detection, 220 and 260 nm), and lyophilized.

Yield: 6.4 mg (62.3%). $R_f = 0.11$ (2-propanol/1 M NH_4OAc, 2:1). $[\alpha]^{22}_D$ −5.6° (*c* 0.78, H_2O). $C_{96}H_{160}N_8O_{66}$ ($M = 2482.33$). ESI-MS: $M_{calcd} = 2480.94$, $M_{found} = 1241.6$ $(M + 2H)^{2+}$.

^{1}H NMR (500 MHz, D_2O/CD_3CN, 9:1): $\delta = 4.93$ (d, $J_{1,2} < 1.0$ Hz, 1H, H-1^A), 4.84 (d, $J_{1,2} = 9.7$ Hz, 1H, H-1^1), 4.75 (d, $J_{1,2} < 1.0$ Hz, 1H, H-1$^{A'}$), 4.68 (d, $J_{1,2} = 3.7$ Hz, 1H, H-1^8), 4.58 (d, $J_{1,2} < 1.0$ Hz, 1H, H-1^3), 4.48 (d, $J_{1,2} = 7.8$ Hz, 1H, H-1^2), 4.41 (d, $J_{1,2} = 7.4$ Hz, 2H, H-1^5, H-1$^{5'}$), 4.24 (d, $J_{1,2} = 7.8$ Hz, 1H, H-1^6), 4.23 (d, $J_{1,2} = 7.8$ Hz, 1H, H-1^6), 4.06 (dd, $J_{2,3} < 1.5$ Hz, 1H, H-2^3), 3.99 (dd, $J_{2,3} = 2.1$ Hz, 1H, H-2^4), 3.92 (m, 2H, H-5^8, H-2$^{4'}$), 3.80−3.26 (m, 64H, H-6a^5, H-6a$^{5'}$, H-4^6, H-4$^{6'}$, H-6a^3, H-6a^4, H-6a$^{4'}$, H-8^N, H-8$^{N'}$, H-3^4, H-3$^{4'}$, H-6a^1, H-9a^N, H-9a$^{N'}$, H-6b^5, H-6b$^{5'}$, H-3^8, H-2^1, H-5^N, H-5$^{N'}$, H-4^8, H-2^8, H-6b^3, H-4^3, H-2^2, H-4^1, H-3^2, H-5^6, H-5$^{6'}$, H-5^4, H-6b^2, H-6a^6, H-6a$^{6'}$, H-6b^6, H-6b$^{6'}$, H-2^5, H-2$^{5'}$, H-3^1, H-4^2, H4^5, H-4$^{5'}$, H-6b^1, H-4^N, H-4$^{N'}$, H-5^1, H-9b^N, H-9b$^{N'}$, H-5^2, H-5^4, H-3^6, H-3$^{6'}$, H-6^N, H-6$^{N'}$, H-6b^4, H-6b$^{4'}$, H-7^N, H-7$^{N'}$, H-5^3, H-2^6, H-2$^{6'}$, H-5^5, H-5$^{5'}$, H-4^4, H-4$^{4'}$), 2.78 (t, $J_{\delta,\epsilon} = 7.6$ Hz, 2H, ϵ-CH_2), 2.48 (dd, $J_{vic} = 4.4$ Hz, $J_{gem} = 12.4$ Hz, 2H, H-3eq^N, H-3eq$^{N'}$), 2.08 (t, $J_{\alpha,\beta} = 7.2$ Hz, 2H, α-CH_2), 1.90, 1.87, 1.86 1.84, 1.83, 1.80 (6s, 18H, NAc), 1.52 (t, $J_{vic} = 12.2$ Hz, 2H, H-3ax^N, H-3ax$^{N'}$), 1.47 (m, 2H, δ-CH_2), 1.40 (m, 2H, β-CH_2), 1.16 (m, 2H, γ-CH_2), 1.01 (d, $J_{5,6} = 6.6$ Hz, 3H, H-6^8).

^{13}C NMR (125 MHz, D_2O/CD_3CN, 9:1): $\delta = 178.18$, 175.79, 175.45, 174.34 C=O, 104.42 C-1^6, C-1$^{6'}$, 101.89 C-1^2, 101.33 C-1^3, 101.06 C-1^4, 100.44 C1^8, 100.29C-1^5, 100.14 C-1$^{5'}$, 97.80 C-1$^{4'}$, 81.57 C-4^5, C-4$^{5'}$, 81.49 C-3^3, 80.60 C-4^2, 79.47C-4^1, 79.21 C-1^1, 77.35 C-2^4, 77.14 C-2$^{4'}$, 76.10 C-5^1, 75.33 C-5^2, C5^5, C-5$^{5'}$, 74.57 C-5^6, C-5$^{6'}$, 74.41 C-5^4, C-3^2, 73.72 C-5$^{4'}$, 73.42 C-3^1, C-5^3, C-6^N, C-6$^{N'}$, 73.32 C-3^6, C-3$^{6'}$, 72.92 C-3^5, C-3$^{5'}$, 72.72 C-4^8, 72.60 C-8^N, C-8$^{N'}$, 71.63 C-2^6, C-2$^{6'}$, 71.06 C-2^3, 70.45 C-3^8, 70.32 C-3^4, C-3$^{4'}$, 69.30 C-4^6, C-4$^{6'}$, C-7^N, C-7$^{N'}$, 69.07 C-2^8, C-4^N, C-4$^{N'}$, 68.22 C-4^4, C-4$^{4'}$, 67.66 C-5^8, C-6^1, 66.76 C-6^3, 66.59 C-4^3, 64.21 C-6^6, C-6$^{6'}$, 63.57 C-9^N, C-9$^{N'}$, 62.49 C-6^4, C-6$^{4'}$, 61.14 C-6^5, C-6$^{5'}$, 60.88 C-6^2, 55.82 C-2^2, 55.54 C-2^5, C-2$^{5'}$, 54.67 C-2^1, 52.78 C-5^N, C-5$^{N'}$, 40.97 C-3^N, C-3$^{N'}$, 40.07 C-6 AH, 36.30 C-2 AH, 27.21 C-5 AH, 25.85 C-4 AH, 25.35 C-3 AH, 23.31, 22.93 NAc, 16.31 C-6^8.

***N*^{1}-(6-Aminohexanoylamido)-*O*-(5-acetamido-3,5-dideoxy-α-D-glycero-D-galacto-2-nonulopyranulosonic acid)-(2→3)-*O*-β-D-galactopyranosyl-(1→4)-*O*-2-acetamido-2-deoxy-β-D-glucopyranosyl-(1→2)-*O*-α-D-mannopyranosyl-(1→3)-*O*-[(5-acetamido-3,5-dideoxy-α-D-glycero-D-galacto-2-nonulopyranulosonic acid)-(2→3)-*O*-β-D-galactopyranosyl-(1→4)-*O*-2-acetamido-2-deoxy-β-D-glucopyranosyl-(1→2)-*O*-α-D-mannopyranosyl-(1→6)]-*O*-β-D-mannopyranosyl-(1→4)-*O*-2-acetamido-2-deoxy-β-D-glucopyranosyl-(1→4)-*O*-[α-L-fucopyranosyl-(1→6)]-2-acetamido-2-deoxy-β-D-glucopyranoside 7 (BiF1223AH).** A 6.5 mg portion (4.12 μmol) of octasaccharide **4** was dissolved in 2.4 mL of a 20 mM sodium cacodylate buffer, pH 7.4. The buffer contained 1.7 mg of bovine serum albumin, 4.34 μmol of NaN_3, 2.43 μmol of $MnCl_2$, 8.3 mg (12.5 μmol) of uridine-5′-diphosphogalactose, 10.3 U of alkaline phosphatase (EC 3.1.3), and 208 mU of GlcNAc-β1,4-galactosyltransferase (EC 2.4.1.22). The reaction mixture was incubated for 48 h at 37 °C. After complete reaction (TLC, 2-propanol/1 M NH_4OAc, 2:1), 7.0 mg (9.1 μmol) of cytidine-5′-monophospho-*N*-acetylneuraminic acid and 75 mU of β-galactoside-α2,3-sialyltransferase (EC 2.4.99.6) were added. After adjustment of the pH to 6.0, incubation at 37 °C was continued for 24 h. A second portion of 7.0 mg (9.1 μmol) of cytidine-5′-monophospho-*N*-acetylneuraminic acid and 75 mU of β-galactoside-α2,6-sialyltransferase were added (pH 6.0). Incubation at 37 °C for 16 h was followed by removal of the precipitate by centrifugation. The supernatant was concentrated to a volume of 450 μL, purified by gel filtration (column, Pharmacia Hi Load Superdex 30, 600 mm × 16 mm; mobile phase, 100 mM NH_4HCO_3; flow rate, 750 μL/min; detection, 220 and 260 nm), and lyophilized.

Yield: 6.5 mg (63.4%). $R_f = 0.12$ (2-propanol/1 M NH_4OAc, 2:1). $[\alpha]^{22}_D$ −5.6° (*c* 0.78, H_2O). $C_{96}H_{160}N_8O_{66}$ ($M = 2482.33$). ESI-MS: $M_{calcd} = 2480.94$, $M_{found} = 1241.6$ $(M + 2H)^{2+}$.

^{1}H NMR (500 MHz, D_2O/CD_3CN, 9:1): $\delta = 4.91$ (d, $J_{1,2} < 1.0$ Hz, 1H, H-1^A α), 4.85 (d, $J_{1,2} = 9.7$ Hz, 1H, H-1^1), 4.73 (d, $J_{1,2} < 1.0$ Hz, 1H, H-1$^{A'}$), 4.68 (d, $J_{1,2} = 3.6$ Hz, 1H, H-1^8), 4.56 (d, $J_{1,2} < 1.0$ Hz, 1H, H-1^3), 4.46 (d, $J_{1,2} = 8.0$ Hz, 1H, H-1^2), 4.37 (d, $J_{1,2} = 7.5$ Hz, 2H, H-1^5, H-1$^{5'}$), 4.35 (d, $J_{1,2} = 8.0$ Hz, 1H, H-1^6), 4.34 (d, $J_{1,2} = 8.0$ Hz, 1H, H-1^6), 4.05 (dd, $J_{2,3} < 1.5$ Hz, 1H, H-2^3), 3.97 (dd, $J_{2,3} = 2.2$ Hz, 1H, H-2^4), 3.92 (m, 4H, H-3^6, H-3$^{6'}$, H-5^8, H-2$^{4'}$), 3.80−3.26 (m, 62H, H-6a^5, H-6a$^{5'}$, H-4^6, H-4$^{6'}$, H-6a^3, H-6a^4, H-6a$^{4'}$, H-8^N, H-8$^{N'}$, H-3^4, H-3$^{4'}$, H-6a^1,

H-9a^{N}, H-9a$^{N'}$, H-6b^{5}, H-6b$^{5'}$, H-3^{8}, H-2^{1}, H-5^{N}, H-5$^{N'}$, H-4^{8}, H-2^{8}, H-6b^{3}, H-4^{3}, H-2^{2}, H-4^{1}, H-3^{2}, H-5^{6}, H-5$^{6'}$, H-5^{4}, H-6b2, H-6a6, H-6a6′, H-6b6, H-6b6′, H-25, H-25′, H-31, H-42, H45, H-45′, H-6b1, H-4N, H-4N′, H-51, H-9bN, H-9bN′, H-52, H-54, H-6N, H-6N′, H-6b4, H-6b4′, H-7N,H-7N′, H-53, H-26, H-26′, H-55, H-55′, H-44, H-44′), 2.79 (t, $J_{\delta,\epsilon}$ = 7.7 Hz, 2H, ϵ-CH2), 2.56 (dd, J_{vic} = 4.4 Hz, J_{gem} = 12.4 Hz, 2H, H-3eq^{N}, H-3eq$^{N'}$), 2.08 (t, $J_{\alpha,\beta}$ = 7.3 Hz, 2H, α-CH_2), 1.90, 1.85, 1.84, 1.83, 1.81 (6s, 18H, NAc), 1.60 (t, J_{vic} = 12.1 Hz, 2H, H-3ax^{N}, H-3ax$^{N'}$), 1.47 (m, 2H, δ-CH_2), 1.38 (m, 2H, β-CH_2), 1.13 (m, 2H, γ-CH_2), 1.01 (d, $J_{5,6}$ = 6.6 Hz, 3H, H-6^{8}).

^{13}C NMR (125 MHz, D_2O/CD_3CN, 9:1): δ = 178.20, 175.90, 175.52, 175.46, 174.71 C=O, 103.55 C-1^{6}, 103.50 C-1$^{6'}$, 101.90 C-1^{2}, 101.28 C-1^{3}, 100.72 C-1^{4}, 100.43 C-1^{5} , C-1$^{5'}$, 100.30 C1^{8}α, 97.96 C-1$^{4'}$, 81.33 C-3^{3}, 80.39 C-4^{2}, 79.45 C-4^{1}, 79.30 C-4^{5}, C-4$^{5'}$, 79.23 C-1^{1}, 77.38 C-2^{4}, 77.20 C-2$^{4'}$, 76.38 C-3^{6}, C-3$^{6'}$, 76.12 C-5^{1}, 76.05 C-3^{5}, C-3$^{5'}$, 75.62 C-5^{5}, C-5$^{5'}$, 75.33 C-5^{3}, 74.43 C-3^{2}, C-5^{4}, 73.78 C-6^{N}, C-6$^{N'}$, C-5^{2}, C-5$^{4'}$, 73.50 C-3^{1}, 72.94 C-5^{6}, 72.79 C-5$^{6'}$, 72.73 C-4^{8}, 72.64 C-8^{N}, C-8$^{N'}$, 71.06 C-2^{3}, 70.46 C-3^{4}, C-3$^{4'}$, C-3^{8}, 70.27 C-2^{6}, C-2$^{6'}$, 69.21 C-4^{N}, C-4$^{N'}$, 69.01 C-2^{8}, C-7^{N}, C-7$^{N'}$, 68.37 C-4^{6}, C-4$^{6'}$, 68.19 C-4^{4}, C-4$^{4'}$, 67.68 C-6^{1}, C-5^{8}, 66.48 C-6^{3}, 65.42 C-4^{3}, 63.50 C-9^{N}, C-9$^{N'}$, 62.53 C-6^{4}, C-6$^{4'}$, 61.90 C-6^{6}, C-6$^{6'}$, 60.87 C-6^{2}, C-6^{5}, C-6$^{5'}$, 55.86 C-2^{2}, 55.74 C-2^{5}, C-2$^{5'}$, 54.68 C-2^{1}, 52.59 C-5^{N}, C-5$^{N'}$, 40.52 C-3^{N}, C-3$^{N'}$, 40.08 C-6 AH, 36.30 C-2 AH, 27.23 C-5 AH, 25.86 C-4 AH, 25.36 C-3 AH, 23.24, 22.92 NAc, 16.31 C-6^{8}.

Synthesis of Neoglycoproteins. A 0.34 μmol portion of each 6-aminohexanoyl-*N*-glycan (**5**−**7**) was dissolved in 200 μL of dilute $NaHCO_3$ (100 mg of Na_2CO_3/10 mL of H_2O) in a 1.5 mL plastic vessel. A solution of 1 μL (13.1 μmol) of thiophosgene in 200 μL of dichloromethane was added, and the biphasic mixture was vigorously stirred. After the amine was consumed (1.5 h, TLC, 2-propanol/1 M ammonium acetate 2:1; R_f value of the decasaccharide derivative = 0.48; R_f value of the α2,3-disialylated derivative = 0.37; R_f of the α2,6-disialylated derivative = 0.28), the phases were separated by centrifugation and the bicarbonate phase was collected. The organic phase was extracted twice with 100 μL of dilute $NaHCO_3$. To remove traces of thiophosgene, the combined aqueous phases were extracted twice with dichloromethane. A 2 mg portion of carbohydrate-free bovine serum albumin was dissolved in the aqueous solution containing the isothiocyanate derivative, and the pH was adjusted to 9.0 by addition of 1 M NaOH. After 6 days at ambient temperature, the neoglycoconjugate was purified by gel filtration (column, Pharmacia Hi Load Superdex 30, 600 mm × 16 mm; mobile phase, 100 mM NH_4HCO_3; flow rate, 750 μL/min; detection, 220 and 260 nm) and the product-containing solution was lyophilized. To calculate the extent of oligosaccharide incorporation into the protein carrier, a colorimetric assay[35] was employed. Gel electrophoretic analysis under denaturing conditions combined with silver staining of the neoglycoproteins was performed, as described.[12] In addition to these three neoglycoproteins, lactosylated albumin was produced by the diazonium and phenylisothiocyanate reactions with *p*-aminophenyl β-lactoside.[34]

Scatchard Analysis in a Solid-Phase Assay. Carbohydrate-dependent binding of biotinylated sugar receptors (galactoside-binding lectins from mistletoe (*Viscum album* L. agglutinin, VAA) and bovine heart (galectin-1) and the β-galactoside-binding immunoglobulin G (IgG) fraction from human serum) to surface-immobilized neoglycoproteins was quantitated in a solid-phase assay in microtiter plate wells, as described in detail previously.[12,47] The experimental series with increasing concentrations of labeled marker and duplicates for each concentration were performed at least four separate times up to saturation of binding, and the data sets were algebraically transformed to obtain the K_D value and the number of bound sugar receptor molecules at saturation.

Flow Cytofluorometry. Automated flow cytofluorometric analysis of carbohydrate-dependent binding of biotinylated marker to the surface of a panel of human tumor cells of different histogenetic origin (BLIN-1, pre-B cell line; Croco II, B-lymphoblastoid cell line; CCRF-CEM, T-lymphoblastoid cell line; K-562, erythroleukemia cell line; KG-1, acute myelogenous leukemia cell line; HL-60, promyelocytic cell line; DU4475, mammary carcinoma cell line; NIH:OVCAR-3: ovarian carcinoma cell line; C205, SW480, and SW620, colon adenocarcinoma cell lines; Hs-294T, melanoma cell line; HS-24, non-small-cell (epidermoid) lung carcinoma cell line) using the streptavidin-*R*-phycoerythrin conjugate as fluorescent indicator (1:40 dilution; Sigma, Munich, FRG) was performed on a FACScan instrument (Becton-Dickinson, Heidelberg, Germany) equipped with the software CONSORT 30, as described previously.[48,49] Biotinylation was performed as described.[12] To reduce nonspecific binding by protein−protein interactions, cells were incubated with 100 μg of ligand-free carrier protein (BSA)/mL for 30 min at 4 °C prior to incubation with the biotinylated neoglycoprotein in Dulbecco's phosphate-buffered saline solution containing 0.1% ligand-free BSA. The extent of non-carbohydrate-dependent fluorescence intensity was subtracted in each case from the total binding.

Glycohistochemical Processing. Following a standard procedure for visualizing carbohydrate-ligand-dependent binding of the neoglycoproteins to sections of bronchial cancer (small cell (18 cases) and the three types of non-small-cell lung cancer (total number of cases: 60; 20 cases for each type), mesothelioma (20 cases), and carcinoid (20 cases)), the specimens were processed under identical conditions with ABC kit reagents and the substrates diaminobenzidine/H_2O_2 for development of the colored, water-insoluble product.[50−52] A case was considered to be positive when at least clusters of tumor cells were specifically stained, and the controls excluded binding of the labeled neoglycoprotein via the protein, the spacer, or the biotin moieties.[50−52] Also, control experiments without the incubation step with the marker ruled out staining by binding of kit reagents, i.e., the glycoproteins avidin or horseradish peroxidase.

Organ Distribution of Radioiodinated Neoglycoproteins. Incorporation of ^{125}I into the neoglycoproteins to reach a specific activity of 11.5 MBq/mg of protein was achieved by the chloramine-T method using limiting amounts of reagents.[53] The retention of radioactivity in Ehrlich solid-tumor-bearing ddY mice (7 weeks old; Nihon Clea Co., Tokyo, Japan) after injection of 28.75 kBq/animal into the tail vain was determined by a γ-counter (Aloka ARC 300, Tokyo, Japan) and expressed as percentage of the injected dose per gram of wet tissue or per milliliter of blood for a group of three to four mice for each type of neoglycoprotein and for each time point, as described.[54,55]

Acknowledgment. We are indebted to Prof. H. Kessler for his support, to Prof. J. C. Paulson and Roche Diagnostics for their generous gifts of reagents, to Dr. S. Namirha for helpful discussion, to B. Hofer for skilfull technical assistance, to the DAAD-NSF exchange program for a travel grant, and to the Deutsche Forschungsgemeinschaft (Grant Un 63/2-2,3), the Leonhard-Lorenz-Stiftung (TUM), the Dr.-M.-Scheel-Stiftung für Krebsforschung, and the Verein zur Förderung des biologisch-technologischen Fortschritts in der Medizin e. V. for financial support.

References

(1) Lee, Y. C.; Lee R. T. Glycobiology in medicine. *J. Biomed. Sci.* **1996**, *3*, 221−237.
(2) Laine, R. A. The information-storing potential of the sugar code. In *Glycosciences: Status and Perspectives*; Gabius, H.-J., Gabius, S., Eds.; Chapman & Hall: London, 1997; pp 1−14.
(3) Gabius, H.-J. Biological information transfer beyond the genetic code: the sugar code. *Naturwissenschaften* **2000**, *87*, 108−121.
(4) Rüdiger, H.; Siebert, H.-C.; Solís, D.; Jiménez-Barbero, J.; Romero, A.; von der Lieth, C.-W.; Diaz-Mauriño, T.; Gabius, H.-J. Medicinal chemistry based on the sugar code: fundamentals of lectinology and experimental strategies with lectins as targets. *Curr. Med. Chem.* **2000**, *7*, 389−416.
(5) Qasba, P. K. Involvement of sugars in protein−protein interactions. *Carbohydr. Polym.* **2000**, *41*, 293−309.

(6) Lee, Y. C.; Townsend, R. R.; Hardy, M. R.; Lönngren, J.; Arnarp, J.; Haraldsson, M.; Lönn, H. Binding of synthetic oligosaccharides to the hepatic Gal/GalNAc lectin. Dependence on fine structural features. *J. Biol. Chem.* **1983**, *258*, 199−202.
(7) Lee, R. T.; Lee, Y. C. Enhanced biochemical affinities of multivalent neoglycoconjugates. In *Neoglycoconjugates. Preparation and Applications*; Lee, Y. C., Lee, R. T., Eds.; Academic Press: San Diego, CA, 1994; pp 23−50.
(8) Mammen, M.; Choi, S.-K.; Whitesides, G. M. Polyvalente Wechselwirkungen in biologischen Systemen: Auswirkungen auf das Design und die Verwendung multivalenter Liganden und Inhibitoren. *Angew. Chem.* **1998**, *110*, 2908−2953.
(9) Yamazaki, N.; Kojima, S.; Bovin, N. V.; André, S.; Gabius, S.; Gabius, H.-J. Endogenous lectins as targets for drug delivery. *Adv. Drug Deliv. Rev.* **2000**, *43*, 225−244.
(10) Gabius, H.-J.; Brinck, U.; Lüsebrink, T.; Ciesiolka, T.; Gabius, S. Glycopeptide−albumin conjugate: its preparation and histochemical ligand properties. *Histochem. J.* **1991**, *23*, 303−311.
(11) Unverzagt, C. Chemoenzymatic synthesis of a sialylated undecasaccharide−asparagine conjugate. *Angew. Chem., Int. Ed.* **1996**, 35, 2350−2353.
(12) André, S.; Unverzagt, C.; Kojima, S.; Dong, X.; Fink, C.; Kayser, K.; Gabius, H.-J. Neoglycoproteins with the synthetic complex biantennary nonasaccharide or its α2,3/α2,6-sialylated derivatives: their preparation, assessment of their ligand properties for purified lectins, for tumor cells in vitro, and in tissue sections, and their biodistribution in tumor-bearing mice. *Bioconjugate Chem.* **1997**, *8*, 845−855.
(13) Brisson, J.-R.; Carver, J. P. The relation of three-dimensional structure to biosynthesis in the N-linked oligosaccharides. *Can. J. Biochem. Cell Biol.* **1983**, *61*, 1067−1078.
(14) Homans, S. W. Conformation and dynamics of oligosaccharides in solution. *Glycobiology* **1993**, *3*, 551−555.
(15) Bush, C. A.; Martin-Pastor, M.; Imberty, A. Structure and conformation of complex carbohydrates of glycoproteins, glycolipids, and bacterial polysaccharides. *Annu. Rev. Biophys. Biomol. Struct.* **1999**, *28*, 269−293.
(16) Dauchez, M.; Mazurier, J.; Montreuil, J.; Spik, G.; Vergoten, G. Molecular dynamics simulations of a monofucosylated biantennary glycan of the *N*-acetyllactosamine type: the human lactotransferrin glycan. *Biochimie* **1992**, *74*, 63−74.
(17) Bourne, Y.; Mazurier, M.; Legrand, D.; Rougé, P.; Montreuil, J.; Spik, G.; Cambillau, C. Structures of a legume lectin complexed with the human lactotransferrin N2 fragment, and with an isolated biantennary glycopeptide: role of the fucose moiety. *Structure* **1994**, *2*, 209−219.
(18) Stubbs, H. J.; Lih, J. J.; Gustafson, T. L.; Rice, K. G. Influence of core fucosylation on the flexibility of a biantennary N-linked oligosaccharide. *Biochemistry* **1996**, *35*, 937−947.
(19) Petrescu, A. J.; Petrescu, S. M.; Dwek, R. A.; Wormald, M. R. A statistical analysis of N- and O-glycan linkage conformations from crystallographic data. *Glycobiology* **1999**, *9*, 343−352.
(20) Kojima, N.; Tachida, Y.; Yoshida, Y.; Tsuji, S. Characterization of mouse ST8Sia II (STX) as a neural cell adhesion molecule-specific polysialic acid synthase. Requirement of core α1,6-linked fucose and a polypeptide chain for polysialylation. *J. Biol. Chem.* **1996**, *271*, 19457−19463.
(21) Suzuki, T.; Kitajima, K.; Inoue, S.; Inoue, Y. Occurrence and potential functions of *N*-glycanases. In *Glycosciences: Status and Perspectives*; Gabius, H.-J., Gabius, S., Eds.; Chapman & Hall: London, 1997; pp 121−131.
(22) Miyoshi, E.; Noda, K.; Ko, J. H.; Ekuni, A.; Kitata, T.; Uozumi, N.; Ikeda, Y.; Matsuura, N.; Sasaki, Y.; Hayashi, N.; Hori, M.; Taniguchi, N. Overexpression of α1,6-fucosyltransferase in hepatoma cells suppresses intrahepatic metastasis after splenic injection in athymic mice. *Cancer Res.* **1999**, *59*, 2237−2243.
(23) Stelck, S.; Robitzki, A.; Willbold, E.; Layer, P. G. Fucose in α-(1−6)-linkage regulates proliferation and histogenesis in reaggregated retinal spheroids of the chick embryo. *Glycobiology* **1999**, *9*, 1171−1179.
(24) Brockhausen, I.; Schutzbach, J.; Kuhns, W. Glycoproteins and their relationship to human disease. *Acta Anat.* **1998**, *161*, 36−78.
(25) Srikrishna, G.; Varki, N. M.; Newell, P. C.; Varki, A.; Freeze, H. H. An IgG monoclonal antibody against Dictyostelium discoideum glycoproteins specifically recognizes Fucα1,6 GlcNAc*β* in the core of *N*-glycans. Localized expression of core-fucosylated glycoconjugates in human tissues. *J. Biol. Chem.* **1997**, *272*, 25743−25752.
(26) Seifert, J.; Lergenmuller, M.; Ito, Y. Synthesis of an α2,3-sialylated, complex-type undecasaccharide. *Angew. Chem., Int. Ed.* **2000**, *39*, 531−534.
(27) (a) Homans, S. W.; Dwek, R. A.; Fernandes, D. L.; Rademacher, T. W. Multiple-step relayed correlation spectroscopy: sequential resonance assignments in oligosaccharides. *Proc. Natl. Acad. Sci. U.S.A.* **1984**, *81*, 6286−6289. (b) Endo, T. Fractionation of glycoprotein-derived oligosaccharides by affinity chromatography using immobilized lectin columns. *J. Chromatogr. A* **1996**, *720*, 251−261. (c) Rice, K. G.; Corradi Da Silva, M. L. Preparative purification of tyrosinamide N-linked oligosaccharides. *J. Chromatogr. A* **1996**, *720*, 235−249.
(28) Unverzagt, C. A modular system for the synthesis of complex *N*-glycans. *Angew. Chem., Int. Ed. Engl.* **1997**, *36*, 1989−1992.
(29) (a) Unverzagt, C.; Seifert, J. Chemoenzymatic synthesis of deca- and dodecasaccharide *N*-glycans of the "bisecting" type. *Tetrahedron Lett.* **2000**, *41*, 4549−4553. (b) Prahl, I.; Unverzagt, C. Synthesis of a LEC14 nonasaccharide, a core-fucosylated, biantennary *N*-glycan with a novel GlcNAc residue in the core region. *Tetrahedron Lett.* **2000**, *41*, 10189−10193.
(30) (a) Unverzagt, C.; Seifert, J. Synthesis of a core-fucosylated, branched octasaccharide as a precursor for glycopeptides of complex *N*-glycans. *Tetrahedron Lett.* **1996**, *37*, 6527−6530. (b)-Seifert, J.; Unverzagt, C. Synthesis of three biantennary *N*-glycans containing the α1,6-core-fucosyl motif. *Tetrahedron Lett.* **1997**, *38*, 7857−7860.
(31) Bayley, H.; Standring, D. N.; Knowles, J. B. Propane-1,3-dithiol; a selective reagent for the efficient reduction of alkyl and aryl azides to amines. *Tetrahedron Lett.* **1978**, *19*, 3633−3634.
(32) Unverzagt, C.; Kunz, H.; Paulson, J. C. High efficiency synthesis of sialyloligosaccharides and sialoglycopeptides. *J. Am. Chem. Soc.* **1990**, *112*, 9308−9309.
(33) Kessler, H.; Gehrke, M.; Griesinger C. Zweidimensionale NMR-Spektroskopie, Grundlagen und Übersicht über die Experimente. *Angew. Chem.* **1988**, *100*, 507−554.
(34) McBroom, C. R.; Samanen, C. H.; Goldstein, I. J. Carbohydrate antigens: coupling of carbohydrates to proteins by diazonium and phenylisothiocyanate reactions. *Methods Enzymol.* **1972**, *28*, 212−219.
(35) Monsigny, M.; Petit, C.; Roche, A.-C. Colorimetric determinations of neutral sugars by a resorcinol sulfuric acid micromethod. *Anal. Biochem.* **1988**, *175*, 525−530.
(36) Eschenburg, S.; Krauspenhaar, R.; Mikhailov, A.; Stoeva, S.; Betzel, C.; Voelter, W. Primary structure and molecular modeling of mistletoe lectin from *Viscum album*. *Biochem. Biophys. Res. Commun.* **1998**, *247*, 367−372.
(37) Sweeney, E. C.; Tonevitsky, A. G.; Palmer, R. A.; Niwa, H.; Pfueller, U.; Eck, J.; Lentzen, H.; Agapov, I. I.; Kirpichnikov, M. P. Mistletoe lectin I forms a double trefoil structure. *FEBS Lett.* **1998**, *431*, 367−370.
(38) Monsigny, M.; Roche, A.-C.; Midoux, P. Uptake of neoglycoproteins via membrane lectin(s) of L1210 cells evidenced by quantitative flow cytofluorometry and drug targeting. *Biol. Cell* **1984**, *51*, 187−198.
(39) Gabius, S.; Joshi, S. S.; Gabius, H.-J.; Sharp, J. G. Establishment, characterization and determination of cell surface sugar receptor (lectin) expression by neoglycoenzymes of a human myeloid-marker-expressing B-lymphoblastoid cell line. *Anticancer Res.* **1991**, *11*, 793−800.
(40) Rogers, J. C.; Kornfeld, S. Hepatic uptake of proteins coupled to fetuin glycopeptide. *Biochem. Biophys. Res. Commun.* **1971**, *45*, 622−629.
(41) Ashwell, G.; Morell, A. G. Membrane glycoproteins and recognition phenomena. *Trends Biochem. Sci.* **1977**, *2*, 76−78.
(42) Saxena, A.; Raveh, L.; Ashani, Y.; Doctor, A. P. Structure of glycan moieties responsible for the extended circulatory life time of fetal bovine serum acetylcholinesterase and equine serum butylcholinesterase. *Biochemistry* **1997**, *36*, 7481−7489.
(43) Chiu, M. H.; Tamura, T.; Wadhwa, M. S.; Rice, K. G. In vivo targeting function of N-linked oligosaccharides with terminating galactose and *N*-acetylgalactosamine residues. *J. Biol. Chem.* **1994**, *269*, 16195−16202.
(44) Gupta, D.; Surolia, A. Synthesis of neoglycopeptides and analyses of their biodistribution in vivo to identify specific uptake and novel putative membrane lectins. *Glycoconjugate J.* **1994**, *11*, 558−571.
(45) Sasayama, S.; Moriya, K.; Chiba, T.; Matsumura, T.; Hayashi, H.; Hayashi, A.; Onozaki, K. Glycosylated human interleukin-1α, neoglyco IL-1α, coupled with *N*-acetylneuraminic acid exhibits selective activities in vivo and altered tissue distribution. *Glycoconjugate J.* **2000**, *17*, 353−359.
(46) Gregoriadis, G.; Fernandes, A.; Mital, M.; McCormack, B. Polysialic acids: potential in improving the stability and pharmacokinetics of proteins and other therapeutics. *Cell. Mol. Life Sci.* **2000**, *57*, 1964−1969.
(47) André, S.; Ortega, P. J. C.; Perez, M. A.; Roy, R.; Gabius, H.-J. Lactose-containing starburst dendrimers: influence of dendrimer generation and binding-site orientation of receptors (plant/animal lectins and immunoglobulins) on binding properties. *Glycobiology* **1999**, *9*, 1253−1261.
(48) Kojima, S.; André, S.; Korchagina, E. Y.; Bovin, N. V.; Gabius, H.-J. Tyramine-containing poly(4-nitrophenylacrylate) as iodinatable ligand carrier in biodistribution analysis. *Pharm. Res.* **1997**, *14*, 879−886.

(49) André, S.; Frisch, B.; Kaltner, H.; Desouza, D. L.; Schuber, F.; Gabius, H.-J. Lectin-mediated drug targeting. Selection of valency, sugar type (Gal/Lac) and spacer length for cluster glycosides as parameters to distinguish ligand binding to C-type asialoglycoprotein receptors and galectins. *Pharm. Res.* **2000**, *17*, 985−990.
(50) Gabius, H.-J.; Bodanowitz, S.; Schauer, A. Endogenous sugar-binding proteins in human breast tissue and benign and malignant breast lesions. *Cancer* **1988**, *61*, 1125−1131.
(51) Kayser, K.; Ziehms, S.; André, S.; Bovin, N. V.; Dong, X.; Kaltner, H.; Gabius, H.-J. Glycohistochemical properties of malignancies of lung and pleura. *Int. J. Oncol.* **1998**, *12*, 1189−1194.
(52) Kayser, K.; Böhm, G.; Blum, S.; Beyer, M.; Zink, S.; André, S.; Gabius, H.-J. Glyco- and immunohistochemical refinement of the differential diagnosis between mesothelioma and metastatic carcinoma and survival analysis of patients. *J. Pathol.* **2001**, *193*, 175−180.
(53) Kojima, S.; Shimura, N.; Kubodera, A.; Takahashi, T.; Oyamada, H. Radioimmunodetection of human colon cancer in nude mice by a new monoclonal antibody A7 against human colorectal cancer. *Nucl. Med. Biol.* **1991**, *18*, 847−853.
(54) Kojima, S.; Gabius, H.-J. Biodistribution of neoglycoproteins in mice bearing solid Ehrlich tumor. *J. Cancer Res. Clin. Oncol.* **1988**, *114*, 468−472.
(55) André, S.; Kojima, S.; Yamazaki, N.; Fink, C.; Kaltner, H.; Kayser, K.; Gabius, H.-J. Galectins-1 and -3 and their ligands in tumor biology. *J. Cancer Res. Clin. Oncol.* **1999**, *125*, 461−474.

JM0110237